

# 1 Immune complex solubility and size govern Fc-gamma receptor responses

2

3 Haizhang Chen<sup>1,2</sup>, Andrea Maul-Pavicic<sup>3,4</sup>, Martin Holzer<sup>5</sup>, Ulrich Salzer<sup>3</sup>, Nina Chevalier<sup>3</sup>,  
4 Reinhard E. Voll<sup>3,4</sup>, Hartmut Hengel<sup>1,2,\*</sup> & Philipp Kolb<sup>1,2,\*</sup>

5

6 <sup>1</sup>Institute of Virology, University Medical Center, Albert-Ludwigs-University Freiburg,  
7 Hermann-Herder-Str. 11, 79104 Freiburg, Germany

8 <sup>2</sup>Faculty of Medicine, Albert-Ludwigs-University Freiburg, 79104 Freiburg, Germany

9 <sup>3</sup>Department of Rheumatology and Clinical Immunology, Medical Center - University of  
10 Freiburg, Faculty of Medicine, University of Freiburg, Hugstetterstr. 55, 79106 Freiburg,  
11 Germany

12 <sup>4</sup>Center for Chronic Immunodeficiency (CCI), Medical Center-University of Freiburg, Faculty  
13 of Medicine, University of Freiburg, Breisacherstr. 115, 79106 Freiburg, Germany

14 <sup>5</sup>Institute for Pharmaceutical Sciences, Albert-Ludwigs-University Freiburg, Hermann-  
15 Herder-Str. 9, 79104 Freiburg, Germany

16

17 \*corresponding authors ([Hartmut.hengel@uniklinik-freiburg.de](mailto:Hartmut.hengel@uniklinik-freiburg.de))

18

19 **One Sentence Summary:** This study reveals selective activation of individual Fc-gamma  
20 receptors by soluble but not immobilized immune complexes, establishing a novel biomarker  
21 for autoimmune disease in humans and mouse models.

22

23

24 **Abstract:** Fc-gamma receptor (Fc $\gamma$ R) activation by soluble IgG immune complexes (sICs) is  
25 thought to be a major mechanism of inflammation in certain autoimmune diseases such as  
26 systemic lupus erythematosus (SLE). A robust and scalable test system allowing for the  
27 detection and quantification of sIC bioactivity is missing. Therefore, we developed a  
28 comprehensive reporter cell panel capable of measuring the sIC-mediated activation of  
29 individual human and mouse Fc $\gamma$ Rs. We show that compared to human Fc $\gamma$ Rs IIB and III,  
30 human Fc $\gamma$ Rs I and IIA lack sensitivity to sICs. Further, the assay proved to be sensitive to  
31 sIC stoichiometry and size enabling us to demonstrate for the first time a complete translation  
32 of the Heidelberger-Kendall precipitation curve to Fc $\gamma$ R responsiveness. This was validated  
33 using primary immune cells. The approach was applied to quantify sIC-mediated Fc $\gamma$ R  
34 activation using sera from SLE patients or from mouse models of lupus and arthritis. Thus, in  
35 clinical practice, it can be employed as a toolbox enabling the evaluation of Fc $\gamma$ R activation  
36 by sICs as a biomarker for disease activity in immune-complex mediated diseases.

37

## 38 **Introduction**

39 Immunoglobulin G (IgG) is the dominant immunoglobulin isotype in chronic infections and  
40 in antibody-mediated autoimmune diseases. The multi-faced effects of the IgG molecule rely  
41 both on the F(ab) regions, which recognize a specific antigen to form immune complexes  
42 (ICs), and the constant Fc region (Fc $\gamma$ ), which is detected by Fc $\gamma$  receptors (Fc $\gamma$ Rs) found on  
43 most cells of the immune system (*1*). When IgG binds to its antigen ICs are formed, which,  
44 depending on the respective antigen, are either cell-bound or soluble (sICs). The composition  
45 of sICs is dependent on the number of epitopes recognized by IgG on a single antigen  
46 molecule and the ability of the antigen to form multimers. Fc $\gamma$ -Fc $\gamma$ R binding is necessary but  
47 not sufficient to activate Fc $\gamma$ Rs since physical receptor cross-linking generally underlies  
48 receptor activation (*2-5*). Firmly fixed cell bound ICs are readily able to cross-link Fc $\gamma$ Rs (*4*,  
49 *6*). This condition induces various signaling pathways (*7-9*) which in turn regulate immune

50 cell effector functions (10, 11). It is also suggested that sICs can dynamically tune Fc $\gamma$ R  
51 triggering, implying that changes in sIC size directly impact Fc $\gamma$ R responses (6). However,  
52 the molecular requirements are largely unknown. Also, a functional reproduction of the  
53 paradigmatic Heidelberger-Kendall precipitation curve, describing that the molecular size of  
54 sICs determined by the antibody:antigen ratio dynamically tunes Fc $\gamma$ R activation on and off  
55 (12, 13), is so far missing.

56 In contrast to Fc $\gamma$ R binding of monomeric ligands without consequences, IC-mediated Fc $\gamma$ R  
57 cross-linking initiates the full signal cascade followed by immune cell activation or inhibition,  
58 resp. (5, 8, 14, 15). Human Fc $\gamma$ Rs are membrane resident receptors recognizing Fc $\gamma$ . Among  
59 all type I Fc $\gamma$ Rs, Fc $\gamma$ RIIB (CD32B) is the only inhibitory one signaling via immunoreceptor  
60 tyrosine-based inhibitory motifs (ITIMs) while the activating receptors are associated with  
61 immunoreceptor tyrosine-based activation motifs (ITAMs). Another exception is Fc $\gamma$ RIIIB  
62 (CD16B), which is glycosylphosphatidylinositol (GPI)-anchored (16-19). Fc $\gamma$ RI (CD64) is the  
63 only receptor with high affinity binding to monomeric IgG not associated with antigen and is  
64 primarily tasked with phagocytosis linked to antigen processing and pathogen clearance (20,  
65 21). All the other Fc $\gamma$ Rs only efficiently bind to complexed, meaning antigen-bound IgG (1,  
66 16, 17). While Fc $\gamma$ RI, Fc $\gamma$ RIIB and Fc $\gamma$ RIIIA are able to recognize sICs, this has not been  
67 reported for Fc $\gamma$ RIIA (CD32A), rather this receptor has recently been shown to depend on the  
68 neonatal Fc receptor (FcRn) or Fc $\gamma$ RIIIB (CD16B) to do so (22, 23). Activation of Fc $\gamma$ Rs  
69 leads to a variety of cellular effector functions such as antibody-dependent cellular  
70 cytotoxicity (ADCC) by natural killer (NK) cells via Fc $\gamma$ RIIIA, antibody-dependent cellular  
71 phagocytosis (ADCP) by macrophages via Fc $\gamma$ RI, cytokine and chemokine secretion by NK  
72 cells and macrophages via Fc $\gamma$ RIIIA. Further effector responses are reactive oxygen species  
73 (ROS) production of neutrophils and neutrophil extracellular traps formation (NETosis) via  
74 Fc $\gamma$ RIIIB, dendritic cell (DC) maturation and antigen presentation via Fc $\gamma$ RIIA and B cell  
75 selection and differentiation via Fc $\gamma$ RIIB (10, 24-30). Consequently, Fc $\gamma$ Rs connect and

76 regulate both innate and adaptive branches of the immune system. Various factors have been  
77 indicated to influence the IC-dependent Fc $\gamma$ R activation profiles, including Fc $\gamma$ -Fc $\gamma$ R binding  
78 affinity and avidity (31), IgG subclass, glycosylation patterns and genetic polymorphism (4,  
79 24, 25, 32), stoichiometry of antigen-antibody-ratio (6, 30, 33) and Fc $\gamma$ R clustering patterns  
80 (34). Specifically, Asn297-linked glycosylation patterns of the IgG Fc domain initiate either  
81 pro- or anti-inflammatory effector pathways by tuning the binding affinity to activating versus  
82 inhibitory Fc $\gamma$ Rs, respectively (35). However, despite being explored in proof-of-concept  
83 studies, the functional consequences of these ligand features on a specific receptor are still not  
84 fully understood. Therefore, an assay platform allowing for the systematic functional  
85 assessment of IC-mediated Fc $\gamma$ R activation is strongly required. While a previously  
86 developed cell-based assay addresses sIC-mediated activation of the inhibitory Fc $\gamma$ RIIB (36),  
87 a platform allowing for the comprehensive analysis of all Fc $\gamma$ Rs is missing.

88 sICs and immobilized ICs represent different stimuli for the immune system (22, 29). Soluble  
89 circulating ICs are commonly associated with certain chronic viral or bacterial infections (37,  
90 38) and autoimmune diseases, such as systemic lupus erythematosus (SLE) or rheumatoid  
91 arthritis (RA) (39-41). When accumulating and deposited in tissues sICs can cause local  
92 damage due to inflammatory responses, classified as type III hypersensitivity (42). Typically,  
93 sICs related disorders are characterized by systemic cytokine secretion which can be followed  
94 by immune cell exhaustion and senescence (43, 44). In order to study sIC-dependent  
95 activation of Fc $\gamma$ Rs in detail, we employed a cell-based assay which has been previously  
96 utilized to study immobilized ICs (45) and adapted it into a sIC sensitive reporter system  
97 capable of distinguishing the activation of individual Fc $\gamma$ Rs and their responses to varying  
98 complex size. This approach allowed for the first time a complete reproduction of the  
99 Heidelberger-Kendall precipitation curve measuring actual Fc $\gamma$ R triggering. The assay  
100 enables a quantification of clinically relevant sICs in sera from SLE patients and autoimmune-

101 prone mice with immune-complex-mediated arthritis and lupus using reporter cells expressing  
102 chimeric mouse Fc $\gamma$ Rs.

103

## 104 **Results**

### 105 *Experimental assay setup*

106 The assay used in this study was adapted from a previously described cell-based Fc $\gamma$ R  
107 activation assay designed to measure receptor activation in response to opsonized virus  
108 infected cells (45) or therapeutic Fc-fusion proteins (46). We complemented the assay setup to  
109 enable measurement of sICs when incubated with reporter cells stably expressing the  
110 ectodomains of the human Fc $\gamma$ R fused to the signaling module of the mouse CD3- $\zeta$  chain  
111 (Fc $\gamma$ RI: Acc# X14356; Fc $\gamma$ RIIA(R): Acc# X62572; Fc $\gamma$ RIIB/C: Acc# X52473; Fc $\gamma$ RIIIA(V):  
112 Acc# LT737365). Ectodomains of Fc $\gamma$ RIIB and Fc $\gamma$ RIIC are identical. Second generation  
113 reporter cells were generated to improve stable expression of chimeric Fc $\gamma$ Rs compared to the  
114 transfectants used in the original assay (45). To this end, BW5147 cells were transduced as  
115 described previously via lentiviral transduction (45, 47). Human Fc $\gamma$ R expression on  
116 transduced cells after puromycin selection is shown in Fig. 1A. Fc $\gamma$ R triggering is translated  
117 into activation of the reporter cells and measured by quantification of endogenous IL-2 (mIL-  
118 2) secretion into the cell culture supernatant using an anti-IL-2 sandwich ELISA as described  
119 previously (45). In order to employ the original assay, designed to detect ICs on adherent  
120 virus-infected cells, for the detection of soluble ICs we first determined the suspension of IgG  
121 achieved by pre-incubating a 96 well ELISA microtiter plate with PBS/FCS blocking buffer.  
122 To this end, we compared graded concentrations of FCS in the blocking reagent and measured  
123 the threshold at which IgG (rituximab, Rtx) was no longer adsorbed to the plate and stayed  
124 abundantly in solution. Fig. 1B demonstrates that FCS supplementation to 1% (v/v) or higher  
125 is sufficient to keep IgG antibodies in solution and prevents binding to the plastic surface.  
126 Using this adapted protocol, the assay now allowed for the sensitive detection and

127 characterization of Fc $\gamma$ R interaction with immobilized ICs versus sICs as shown  
128 schematically in Fig. 1C. First, we set out to test if monomeric IgG upon immobilization  
129 becomes an operational surrogate for IgG-opsonized cells or immobilized ICs with regard to  
130 Fc $\gamma$ R activation as suggested before (48). As depicted in Fig. 2, there was no qualitative  
131 difference in Fc $\gamma$ R activation between immobilized Rtx, immobilized ICs (Rtx + rec. CD20)  
132 or Rtx-opsonized 293T-CD20 cells, showing that Fc $\gamma$ R cross-linking by clustered IgG alone is  
133 sufficient for receptor cross-linking and activation. In contrast, sICs formed by monomeric  
134 CD20 peptide (aa 141-188) and Rtx failed to activate Fc $\gamma$ Rs even at very high ligand  
135 concentrations. Based on this finding we hypothesized that, in order to generate sICs able to  
136 activate Fc $\gamma$ Rs, antigens have to be multivalent to achieve cross-linking of Fc $\gamma$ Rs. Of note, to  
137 reliably and accurately differentiate between soluble and immobilized triggers using this  
138 assay, reagents for the generation of ICs need to be of very high purity and consistent  
139 stability. Indeed, only combinations of pharmaceutical therapy grade, i.e. ultra-pure mAbs and  
140 pure antigens (purified via size exclusion chromatography) showed reproducible, dose-  
141 dependent and specific activation in the reporter assay (data not shown).

142

#### 143 *Quantification of human Fc $\gamma$ R responsiveness to multimeric sICs*

144 To date, there are only few commercially available human IgG-antigen pairs that meet both  
145 the above mentioned high grade purity requirements while also providing a multimeric  
146 antigen. In order to meet these stipulations of ultra-pure synthetic soluble immune complexes  
147 we focused on three pairs of multivalent antigens and their respective mAbs that were  
148 available in required amounts enabling large-scale titration experiments; trimeric  
149 rhTNF $\alpha$ :IgG1 infliximab (TNF $\alpha$ :Ifx), dimeric rhVEGFA: IgG1 bevacizumab (VEGFA/Bvz)  
150 and dimeric rhIL-5: IgG1 mepolizumab (IL-5/Mpz). As lymphocytes express TNF $\alpha$ -receptors  
151 I and II while not expressing receptors for IL-5 or VEGFA, we tested whether the mouse  
152 lymphocyte derived BW5147 thymoma reporter cell line is sensitive to high concentrations of

153 rhTNF $\alpha$ . Toxicity testing revealed that even high concentrations up to 76.75 nM rhTNF $\alpha$  did  
154 not affect viability of reporter cells (Fig. S1). Next, we measured the dose-dependent  
155 activation of human Fc $\gamma$ R<sub>s</sub> comparing immobilized IgG to soluble ICs using the Fc $\gamma$ R  
156 reporter cell panel (Fig. 3). Soluble antigen or mAb alone served as negative controls showing  
157 no background activation even at high concentrations. Immobilized rituximab served as a  
158 positive control for inter-experimental reference. We observed that all Fc $\gamma$ R<sub>s</sub> are strongly  
159 activated in a dose-dependent manner when incubated with immobilized IgG. Incubating the  
160 Fc $\gamma$ R reporter cells with sICs at identical molarities showed Fc $\gamma$ R<sub>IIIB/C</sub> and Fc $\gamma$ R<sub>IIIA</sub> to be  
161 efficiently activated by sICs, while in contrast, Fc $\gamma$ R<sub>IIA</sub> and Fc $\gamma$ R<sub>I</sub> did not respond to sICs.  
162 We furthermore observed Fc $\gamma$ R<sub>IIIA</sub> to be efficiently activated by sICs with responses even  
163 surpassing those achieved with immobilized IgG for TNF $\alpha$ /I $\alpha$ x and IL-5/Mp $\zeta$  ICs. Fc $\gamma$ R<sub>IIIB/C</sub>  
164 showed a generally weaker reactivity towards sICs compared to immobilized ICs, especially  
165 at high concentrations whereas an inversion of this order was seen for TNF $\alpha$ /I $\alpha$ x and  
166 VEGFA/Bv $\zeta$  ICs at lower concentrations. IL-5/Mp $\zeta$ , Fc $\gamma$ R<sub>IIIB/C</sub> and Fc $\gamma$ R<sub>IIIA</sub> showed  
167 similar responsiveness towards immobilized or sICs with a generally stronger activation on  
168 immobilized ICs. These findings demonstrate that sICs of different composition vary in the  
169 resulting Fc $\gamma$ R activation pattern, most likely due to the antigens being either dimeric, trimeric  
170 or different in size. As we observed differences in responses to sICs vs. immobilized ICs for  
171 individual Fc $\gamma$ R- $\zeta$  reporter cells, this indicates that Fc $\gamma$ R ectodomains alone are already able  
172 to differentiate between these triggers. To validate this observation in principle, we  
173 determined Fc $\gamma$ R<sub>IIIA</sub> activation using primary human NK cells isolated from PBMCs of  
174 healthy donors. NK cells were chosen as they mostly express only one type of Fc $\gamma$ R similar to  
175 our reporter system. Measuring a panel of activation markers and cytokine responses by flow  
176 cytometry, we observed a differential activation pattern depending on ICs being soluble or  
177 immobilized at equal molarity (Fig. 4A). We chose IL-5/Mp $\zeta$  sICs as NK cells do not express  
178 the IL-5 receptor. While MIP1- $\beta$  responses were comparable between the two triggers,

179 degranulation (CD107a) and TNF $\alpha$  responses showed a trend towards lower activation by  
180 sICs compared to immobilized IgG (Mpz). Strikingly, IFN $\gamma$  responses were significantly  
181 weaker when NK cells were incubated with sICs compared to immobilized IgG. In order to  
182 confirm this hierarchy of responses and to enhance the overall low activation by Fc $\gamma$   
183 compared to the PMA control, we changed the IC setup by generating reverse-orientation  
184 sICs consisting of human Fc $\gamma$ R-specific mouse mAbs and goat-anti-mouse IgG F(ab)<sub>2</sub>  
185 fragments. NK cell activation by reverse sICs was compared to NK cell activation by  
186 immobilized Fc $\gamma$ R specific mAbs (Fig. 4B). Here, we not only confirm our previous  
187 observations regarding MIP-1 $\beta$  and IFN $\gamma$ , but we also confirm significantly lower TNF $\alpha$  and  
188 CD107a responses towards soluble complexes compared to immobilized mAbs. Importantly,  
189 these experiments validate that sICs readily activate primary NK cells and induce  
190 immunological effector functions. As in roughly 10% of the population NK cells express  
191 Fc $\gamma$ RIIC (49-52), we also tested if this receptor plays a role in our measurements. Using the  
192 same three donors and an Fc $\gamma$ RII specific mAb as described above, we did not observe an  
193 Fc $\gamma$ RII-mediated response. Accordingly, we conclude that Fc $\gamma$ RIIC expression did not play a  
194 role in our experiments (Fig. 4C). Taken together, we show that multivalent but not dimeric  
195 soluble immune complexes govern primary NK cell response and Fc $\gamma$ RIIIA activation (Fig.  
196 2A).

197

#### 198 *Measurement of Fc $\gamma$ R activation in response to changing sIC size*

199 We observed that the dimeric sIC CD20:Rtx molecule complex completely failed to trigger  
200 Fc $\gamma$ Rs, while potentially larger sICs based on multimeric antigens showed an efficient dose-  
201 dependent Fc $\gamma$ R activation. In order to determine whether BW5147 Fc $\gamma$ R- $\zeta$  reporter cells are  
202 able to respond to changes in sIC size, we tested cross-titrated amounts of antibody (mAb,  
203 infliximab, Ifx) and antigen (Ag, rhTNF $\alpha$ ). To this end, the reporter cells were incubated with  
204 sIC of different mAb:Ag ratios by fixing one parameter and titrating the other. According to



205 the Heidelberger-Kendall precipitation curve (12) describing sIC size as being dependent on  
206 the mAb:Ag ratio, this should result in varying sIC sizes as an excess of either antigen or  
207 antibody results in the formation of smaller complexes compared to the large molecular  
208 complexes formed at around equal molarity. Changes in sIC size due to a varying mAb:Ag  
209 ratio were quantified using asymmetrical flow-field flow fractionation (AF4) (Fig. 5A and  
210 Table S1). Fig. S2 shows a complete run of such an analysis. AF4 analysis identifies the  
211 highest sIC mean molecular being approximately 2130 kDa at a 1:3 ratio (mAb Ix : Ag TNF-  
212  $\alpha$ ) with sICs getting smaller with increasing excess of either antigen or antibody,  
213 recapitulating a Heidelberger-Kendall-like curve. Incubation of the Fc $\gamma$ R reporter cells with  
214 ICs of varying size indeed shows that the assay is sensitive to exactly monitor changes in sIC  
215 size (Fig. 5B). Accordingly, both Fc $\gamma$ R types showed the strongest responses at mAb:Ag  
216 ratios of approximately 1:3. We then set out to test the accuracy of our reporter cell assay as a  
217 surrogate for primary human immune cells expressing Fc $\gamma$ Rs. To this end, we tested primary  
218 NK cells from three individual donors and measured NK cell MIP1- $\beta$  upregulation in  
219 response to synthetic sICs of varying size and composition again using a similar assay setup  
220 optimized for NK cell activation. We chose MIP-1 $\beta$  upregulation as a cell surface marker to  
221 measure NK cell activation as it showed the highest responsiveness in previous experiments  
222 (Fig. 4). We could observe that primary immune cells expressing Fc $\gamma$ RIIIA respond to IC  
223 size, confirming our assay to be an accurate surrogate for primary immune cell responses to  
224 soluble ICs (Fig. 5C). Convincingly, NK cell responses to sICs generated from trimeric  
225 antigen (rhTNF $\alpha$ ) peaked at a different mAb:Ag ratio compared to NK cell responses to sICs  
226 generated from dimeric antigens (rhIL-5 and rhVEGFA). Of note, TNF $\alpha$  and VEGFA activate  
227 resting NK cells thus leading to higher MIP1- $\beta$  positivity when NK cells are incubated in the  
228 presence of excess antigen. As NK cells do not express IL-5 receptor, this effect is not  
229 observed in the presence of excess IL-5. Regarding TNF $\alpha$ , NK cells still show a stronger  
230 activation by sICs generated under optimal mAb:Ag ratios compared to conditions where

231 excess antigen is used. The data reveal a direct correlation between sIC size and effector  
232 responses. Conversely, when changing antibody concentrations using fixed amounts of  
233 antigen, a consistent reduction of NK cell activation is observed in the presence of excess IgG  
234 for all three mAb/Ag pairs.

235

### 236 *Quantification of sIC bioactivity in sera of SLE patients*

237 In order to apply the assay to a clinically relevant condition associated with the occurrence of  
238 sICs we measured circulating sICs present in the serum of SLE patients with variable disease  
239 activity. Sera from 4 healthy donors and 25 SLE patients were investigated for Fc $\gamma$ RIIIA and  
240 Fc $\gamma$ RIIB/C activation. Reporter cells readily produced IL-2 in response to patient sera in a  
241 dose-dependent manner (shown exemplarily for some SLE patients, see Fig. 6A), which was  
242 not the case when sera from healthy controls were tested. Consistent with the observation that  
243 Fc $\gamma$ RI and Fc $\gamma$ RIIA do not respond to synthetic sICs, reporter cells expressing these receptors  
244 did also not respond to the tested serum samples (Fig. 6A, lower panel). While this reaction  
245 pattern already indicated that sICs are the reactive component measured in SLE patients' sera,  
246 we further demonstrate that Fc $\gamma$ RIIIA and Fc $\gamma$ RIIB/C activation depends on the presence of  
247 serum ICs by analyzing patient serum before and after polyethylene glycol (PEG)  
248 precipitation and depletion of sICs (Fig. 6B). Next, we calculated the area under the curve  
249 (AUC) values for all 25 SLE patient titrations and normalized them to the AUC values  
250 measured for healthy individuals. The resulting index values were then correlated with  
251 established biomarkers of SLE disease activity, such as anti-dsDNA titers ( $\alpha$ -dsDNA) and  
252 concentrations of the complement cleavage product C3d (Fig. 6C). We observed a significant  
253 correlation between our Fc $\gamma$ RIIIA activation index values and both of the determined disease  
254 activity markers, anti-dsDNA titers and C3d concentration ( $p=0.0465$  and  $p=0.0052$ ,  
255 respectively). Fc $\gamma$ RIIB/C on the other hand showed no significant correlation with either  
256 biomarker. We assume these interrelations may be due to the influence of IgG sialylation

257 found to be reduced in active SLE (53). Generally, de-sialylation of IgG leads to stronger  
258 binding by the activating receptors FcγRI, FcγRIIA and FcγRIII while it reduces the binding  
259 affinity of the inhibitory FcγRIIB (54). In sum, our assay allows the indirect quantification of  
260 clinically relevant sICs in sera of SLE patients.

261

#### 262 *Assay application to clinically relevant in vivo lupus and arthritis mouse models*

263 BW5147 reporter cells stably expressing chimeric mouse as well as rhesus macaque FcγRs  
264 have already been generated using the here described methodology and were successfully  
265 used to measure FcγR activation by opsonized adherent cells in previous studies (47, 55)  
266 (mFcγR reporter cells). As the human FcγR reporter cells described here are sensitive to  
267 certain sICs, we next aimed to translate the assay to clinically relevant animal models. To this  
268 end, we incubated previously described FcγR reporter cells expressing chimeric mouse FcγRs  
269 (47) with sera from lupus (NZB/WF1) or arthritis (K/BxN) mice with active autoimmune  
270 disease. The reporter assay was performed as described above. We chose to measure the  
271 stimulation of the activating receptors, mFcγRIII and mFcγRIV, that correspond to human  
272 FcγRIII and show a similar cellular distribution and immune function (16). Incubation with  
273 synthetic sICs generated from rhTNFα and mouse-anti-hTNFα IgG1 showed both of the  
274 mFcγR reporter cells to be equally responsive to sICs (Fig. 7A). Parental BW5147 cells  
275 expressing no FcγRs served as a control. The sera of three mice per group were analysed and  
276 compared to sera from wildtype C57BL/6 mice, which served as a healthy control. C57BL/6  
277 mice were chosen, as healthy K/BxN or NZB/WF1 mice cannot be reliably defined. This is  
278 due to the unpredictable disease progression in these mouse models starting from a young age.  
279 We consistently detected mFcγR activation by sera from K/BxN or NZB/WF1 compared to  
280 C57BL6 mice (Fig. 7B). While the mFcγRIII responses were generally high and similar  
281 between K/BxN and NZB/WF1 mice, mFcγRIV responsiveness attended to be lower and  
282 individually more variable. Altogether, the assay enables the reliable detection of sICs in sera

283 of mice with immune-complex mediated diseases making it a promising novel tool to monitor  
284 sICs as a biomarker of disease activity.

285

## 286 **Discussion**

287 In this study we established, validated and applied a new assay system that is able for the first  
288 time to selectively detect soluble multimeric immune complexes as discrete ligands of Fc $\gamma$ R.  
289 Major findings are i) that sICs cross-link and trigger human Fc $\gamma$ Rs IIB/C and IIIA but are  
290 neglected by activating Fc $\gamma$ RI and IIA; ii) that sICs potency is strictly stoichiometry- and size-  
291 dependent and thus reproducing the classical Heidelberger-Kendall curve iii) that the overall  
292 functional design of Fc $\gamma$ Rs is adapted to physical cross-linking by soluble vs. membrane-  
293 bound immune complexes. The new test system has various obvious applications in medicine  
294 and pharmacy.

295

### 296 *A novel assay for the quantification of disease-associated as well as synthetic sICs*

297 The new approach presents an important and implementable advancement in immunological  
298 methodology as it enables the sensitive detection of receptor-activating ICs by a relatively  
299 simple, scalable *in vitro* bioassay with high-throughput potential. Based on our pilot study  
300 demonstrating that the sIC-mediated Fc $\gamma$ RIIIA activation correlated with SLE disease  
301 markers, this is of great value for larger prospective clinical studies in patients with  
302 autoimmune diseases such as systemic lupus erythematosus (SLE) and rheumatoid arthritis  
303 (RA), where circulating ICs have long been shown to crucially contribute to tissue damage  
304 and disease manifestations (40, 41, 56-58). Disease-associated, endogenous sICs can also  
305 occur during infection, e.g. generated after antibody-mediated destruction of pathogenic  
306 viruses or microbes or probably more likely due to the oligomeric nature of numerous viral  
307 and bacterial structural proteins generated e.g. by SARS-CoV2 (59-61) HIV and hepatitis B  
308 virus (HBV) infection, during which circulating sICs are generated (37, 62). As the assay also

309 enables the sensitive and quantitative measurement of Fc $\gamma$ R ligand bioactivity it allows the  
310 detection of sICs not only in clinical specimens but also pharmaceutical preparations of IgG  
311 and Fc-fusion proteins for therapeutic use (46). The presence of ICs in therapeutic  
312 preparations or sIC formation following patient treatment is unwanted due to the risk of side  
313 effects such as lupus-like syndrome which has been linked to mAb treatment in patients  
314 receiving infliximab (63) or bevacizumab (64), both mAbs used in this study. As this assay is  
315 highly sensitive to any aggregation of IgG, it also represents a tool to control the purity,  
316 quality and stability of mAb preparations produced for therapeutic use in patients. In addition,  
317 the assessment of sIC-mediated Fc $\gamma$ R activation allows for optimization of mAbs and Fc-  
318 fusion proteins regarding their molecular design and manufacturing. Specifically, Fc-  
319 molecules targeting cytokines and soluble factors, which result in sIC formation, could be  
320 designed for reduced or enhanced Fc $\gamma$ R activation such as glyco-engineered mAbs or LALA-  
321 mutant mAbs (65, 66). Notably, the scalability of this cell-based test system does allow for  
322 large-scale screening of samples.

323

#### 324 *sICs form Fc $\gamma$ R ligands with distinct functional profiles*

325 While immobilized ICs decorating infected cells, viral particles or microbial surfaces restrict  
326 their triggering effect to a single immune cell residing in very close vicinity, sICs can rapidly  
327 disseminate reaching a high number of immune effector cells thus developing a systemic  
328 effect with far reaching and long-lasting or even threatening consequences for the host as a  
329 whole. This could explain the very tight control of sIC governed effector programs and the  
330 unresponsiveness of activating receptors like Fc $\gamma$ RI and IIA. We also observed a difference in  
331 the response patterns for Fc $\gamma$ RIIIA and Fc $\gamma$ RII/B/C depending on the solubility of clustered  
332 IgG (immobilized versus soluble ICs) which we validated for Fc $\gamma$ RIIIA using primary human  
333 NK cells (Fig. 4 and 5C). Importantly, only multimeric but not dimeric sICs can trigger Fc $\gamma$ R  
334 activation. This highlights the fundamental structural influence of the particular antigen as

335 well as the IgG molecule on sIC dimension and subsequent FcγR-mediated signal processing.  
336 The ability of the here described assay to define and quantify the activation of individual  
337 FcγRs by sIC ligands is not achievable using primary immune cells due to redundant immune  
338 responses upon FcγR activation and complex, overlapping expression pattern of FcγRs.  
339 Finally, and in contrast to primary human cells, murine BW5147 reporter cells are largely  
340 inert to human cytokines, which provides a key advantage to measure FcγR activation  
341 selectively in human samples. Notably, the two basically sIC-responsive human FcγR types,  
342 i.e. FcγRIIIA and FcγRIIB, are either highly activating versus strongly inhibitory and thus  
343 show a mutually exclusive expression pattern (ref. review, z.B. Ravetch und Falk). FcγRIIIA  
344 mediates ADCC elicited by NK cells and the induction of a pro-inflammatory cytokine profile  
345 by CD16<sup>+</sup> monocytes, while FcγRIIB is a GPI-anchored receptor on neutrophils. FcγRIIB is  
346 an inhibitory receptor expressed by B cells and dendritic cells (DCs) regulating B cell  
347 activation, antibody production by plasma cells and the activation state of DCs, while the  
348 activating FcγRIIC is found on NK cells mediating ADCC. However, as FcγRIIC is only  
349 expressed by roughly 10% of the human population, its role is still poorly understood (49-52).  
350 Given the here shown fundamental difference in FcγR reactivity towards multimeric sICs  
351 versus immobilized IgG it is tempting to speculate that FcγRIIIA- and FcγRIIB/C-positive  
352 immune cells might have evolved to differentially perceive these different FcγR ligands (sICs  
353 versus membrane bound insoluble ICs) and translate them into distinct reaction patterns. This  
354 could be achieved by differences in receptor density, signal transduction or regulation of  
355 receptor expression. Consulting the literature indeed supports our hypothesis with neutrophils,  
356 B cells and NK cells being efficiently activated by sICs via almost identical receptor  
357 ectodomains (18, 28, 67, 68), while the immunological outcome of their triggering very much  
358 differs.  
359  
360

361

362 *Dynamic sIC size measurement and monitoring of bioactivity in sIC-associated diseases*

363 We provide for the first time a simultaneous functional and biophysical assessment of the  
364 paradigmatic Heidelberger-Kendall precipitation curve (12, 13). While previous work already  
365 revealed that large and small sICs differentially impacts IL-6 production in PBMCs (6), the  
366 dynamics of Fc $\gamma$ R activation resulting from constant changes in sIC size have not been  
367 explored on a systematic basis. This was undertaken in this study by directly analyzing  
368 synthetic ICs formed by highly pure recombinant components via AF4 (Fig. 5A, Fig. S2,  
369 Table S1). Our data document that sIC size is indeed governed by antibody:antigen ratios  
370 covering a wide range of sizes up to several megadaltons. In the presence of increasing  
371 amounts of antibody or antigen deviating from an optimal antibody:ratio, sIC size steadily  
372 decreases. Further, by the measurement of Fc $\gamma$ R activation we now translate sIC size directly  
373 to a simple but precise read-out. In doing so, we show that sIC size essentially tunes Fc $\gamma$ R  
374 activation on and off. Thus, our new test system can not only contribute to the functional  
375 detection and quantification of clinically relevant sICs but also provides a starting point on  
376 how to avoid pathological consequences by influencing the sIC size, for example by  
377 administering therapeutic antibodies or recombinant antigens in optimized concentrations,  
378 thus becoming relevant in clinical pharmacokinetics.

379

380 *Limitations of the reporter system and conclusions*

381 While it is known that Fc $\gamma$ RIIA requires Fc $\gamma$ RIIIB or FcRn to efficiently respond to ICs (22,  
382 23, 69), unexpectedly, we found that Fc $\gamma$ RI is not activated by sICs in our assay. We assume  
383 that Fc $\gamma$ RI interaction with sICs might require a native cellular environment given that a  
384 major function of this Fc $\gamma$ R is the uptake and processing of antigen via ICs even in the  
385 absence of a signaling motif (21). However, we find that Fc $\gamma$ RI ectodomains alone are not  
386 responsive to sICs implying a thoroughly different cross-linking threshold for Fc $\gamma$ RI

387 compared with Fc $\gamma$ RIIB and IIIA. This feature is possibly linked to its molecular architecture  
388 being the only high-affinity Fc $\gamma$ R with three extracellular Ig domains compared to the two  
389 domains found in other Fc $\gamma$ Rs with lower affinity to monomeric IgG. This observation also  
390 reflects a general consideration regarding the BW5147 reporter system. While providing a  
391 robust and uniform read-out using a scalable cell-based approach, the assay is not able to  
392 reflect native immune cell functions governed by cell-intrinsic signalling cascades. The major  
393 advancements of this reporter system include i) a higher accuracy regarding Fc $\gamma$ R activation  
394 compared to merely affinity measurements, ii) an sIC size dependent quantification of Fc $\gamma$ R  
395 responsiveness and iii) the identification of Fc $\gamma$ R activating sICs in autoimmunity and  
396 infection. Finally, this scalable, sensitive and robust system to detect Fc $\gamma$ R activating sICs in  
397 clinical samples might enable their identification in diseases that have not been linked to sIC-  
398 mediated pathology, yet.

399

## 400 **Materials and Methods**

401

402 *Cell culture:* All cells were cultured in a 5% CO<sub>2</sub> atmosphere at 37°C. BW5147 mouse  
403 thymoma cells (BW, obtained from ATCC: TIB-47) were maintained at 3x10<sup>5</sup> to 9x10<sup>5</sup>  
404 cells/ml in Roswell Park Memorial Institute medium (RPMI GlutaMAX, Gibco)  
405 supplemented with 10% (vol/vol) fetal calf serum (FCS, Biochrom), sodium pyruvate (1x,  
406 Gibco) and  $\beta$ -mercaptoethanol (0.1 mM, Gibco). 293T-CD20 (kindly provided by Irvin Chen,  
407 UCLA (70)) were maintained in Dulbecco's modified Eagle's medium (DMEM, Gibco)  
408 supplemented with 10% (vol/vol) FCS.

409

410 *Fc $\gamma$ R receptor activation assay:* Fc $\gamma$ R activation was measured adapting a previously  
411 described cell-based assay (45, 71). The assay was modified to measure Fc $\gamma$ R activation in  
412 solution. Briefly, 2x10<sup>5</sup> mouse BW-Fc $\gamma$ R (BW5147) reporter cells were incubated with



413 synthetic sICs or diluted serum in a total volume of 100  $\mu$ l for 16 h at 37°C and 5% CO<sub>2</sub>.  
414 Incubation was performed in a 96-well ELISA plate (Nunc maxisorp) pre-treated with  
415 PBS/10% FCS (v/v) for 1 h at 4°C. Immobilized IgG was incubated in PBS on the plates prior  
416 to PBS/10% FCS treatment. Reporter cell mIL-2 secretion was quantified via ELISA as  
417 described (45).

418  
419 *Recombinant antigens and monoclonal antibodies to form sICs:* Recombinant human (rh)  
420 cytokines TNF, IL-5, and VEGFA were obtained from Stem Cell technologies. Recombinant  
421 CD20 was obtained as a peptide (aa141-188) containing the binding region of rituximab  
422 (Creative Biolabs). Fc $\gamma$ R-specific mAbs were obtained from Stem Cell technologies (CD16:  
423 clone 3G8; CD32: IV.3). Reverse sICs were generated from these receptor-specific antibodies  
424 using goat-anti-mouse IgG F(ab)<sub>2</sub> fragments (Invitrogen) in a 1:1 ratio. Pharmaceutically  
425 produced humanized monoclonal IgG1 antibodies infliximab (Ifx), bevacizumab (Bvz),  
426 mepolizumab (Mpz) and rituximab (Rtx) were obtained from the University Hospital  
427 Pharmacy Freiburg. Mouse anti-hTNF $\alpha$  (IgG2b, R&D Systems, 983003) was used to generate  
428 sICs reactive with mouse Fc $\gamma$ Rs. sICs were generated by incubation of antigens and  
429 antibodies in reporter cell medium or PBS for 2 h at 37°C.

430  
431 *Lentiviral transduction:* Lentiviral transduction of BW5147 cells was performed as described  
432 previously (47, 55). In brief, chimeric Fc $\gamma$ R-CD3 $\zeta$  constructs (45) were cloned into a  
433 pUC2CL6IPwo plasmid backbone. For every construct, one 10-cm dish of packaging cell line  
434 at roughly 70% density was transfected with the target construct and two supplementing  
435 vectors providing the VSV gag/pol and VSV-G-env proteins (6  $\mu$ g of DNA each) using  
436 polyethylenimine (22.5  $\mu$ g/ml, Sigma) and Polybrene (4  $\mu$ g/ml; Merck Millipore) in a total  
437 volume of 7 ml (2 ml of a 15-min-preincubated transfection mix in serum-free DMEM added  
438 to 5 ml of fresh full DMEM). After a medium change, virus supernatant harvested from the

439 packaging cell line 2 days after transfection was then incubated with target BW cells  
440 overnight (3.5 ml of supernatant on  $10^6$  target cells), followed by expansion and pool  
441 selection using complete medium supplemented with 2  $\mu\text{g}/\text{ml}$  of puromycin (Sigma) over a  
442 one week culture period.

443  
444 *BW5147 toxicity test:* Cell counting was performed using a Countess II (Life Technologies)  
445 according to supplier instructions. Cell toxicity was measured as a ratio between live and dead  
446 cells judged by trypan blue staining over a 16 h time frame in a 96well format (100  $\mu\text{l}$  volume  
447 per well). BW5147 cells were mixed 1:1 with Trypan blue (Invitrogen) and analysed using a  
448 Countess II. rhTNF $\alpha$  was diluted in complete medium.

449  
450 *human IgG suspension ELISA:* 1  $\mu\text{g}$  of IgG1 (rituximab in PBS, 50  $\mu\text{l}/\text{well}$ ) per well was  
451 incubated on a 96well microtiter plate (NUNC Maxisorp) pre-treated (2h at RT) with PBS  
452 supplemented with varying percentages (v/v) of FCS (PAN Biotech). IgG1 bound to the  
453 plates was detected using an HRP-conjugated mouse-anti-human IgG mAb (Jackson  
454 ImmunoResearch).

455  
456 *BW5147 cell flow cytometry:* BW5147 cells were harvested by centrifugation at 900 g and RT  
457 from the suspension culture.  $1 \times 10^6$  cells were stained with PE- or FITC-conjugated anti-  
458 human Fc $\gamma$ R mAbs (BD) or a PE-TexasRed-conjugated human IgG-Fc fragment (Rockland)  
459 for 1h at 4°C in PBS/3%FCS. After 3 washing steps in PBS/3%FCS, the cells were  
460 transferred to Flow cytometry tubes (BD) and analysed using BD LSR Fortessa and FlowJo  
461 (V10) software.

462  
463 *NK cell activation flow cytometry:* PBMC were purified from donor blood using Lymphocyte  
464 separation Media (Anprotec). Primary NK cells were separated from donor PBMCs via

465 magnetic bead negative selection (Stem Cell technologies) and NK cell purity was confirmed  
466 via staining of CD3 (Biolegend, clone HIT3a), CD16 (Biolegend, clone 3G8) and CD56  
467 (Miltenyi Biotec, clone AF12-7H3). 96well ELISA plates (Nunc Maxisorp) were pre-treated  
468 with PBS/10% FCS (v/v) for 1 h at 4°C. NK cells were stimulated in pre-treated plates and  
469 incubated at 37°C and 5% CO<sub>2</sub> for 4 h. Golgi Plug and Golgi Stop solutions (BD) were added  
470 as suggested by supplier. CD107a (APC, BD, H4A3) specific conjugated mAb was added at  
471 the beginning of the incubation period. Following the stimulation period, MIP-1β (PE, BD  
472 Pharmigen), IFNγ (BV-510, Biolegends, 4SB3) and TNFα (PE/Cy7, Biolegends, MAB11)  
473 production was measured via intracellular staining Cytokines (BD, CytoFix/CytoPerm, Kit as  
474 suggested by the supplier). 50 ng/ml PMA (InvivoGen) + 0.5 μM Ionomycin (InvivoGen)  
475 were used as a positive stimulation control for NK cell activation. After 3 washing steps in  
476 PBS/3%FCS, the cells were transferred to Flow cytometry tubes (BD) and analysed using a  
477 BD FACS Fortessa and FlowJo (V10) software. FcγRII or FcγRIII block was performed by  
478 addition of receptor specific mAbs (Stem cell technologies, IV.3 and 3G8) at a 1:100 dilution  
479 at the beginning of the incubation period. Cells were transferred to Flow cytometry tubes  
480 (BD) and analyzed using BD LSR Fortessa and FlowJo (V10) software.

481  
482 *Asymmetric flow field flow fractionation (AF4)*: The AF4 system consisted of a flow  
483 controller (Eclipse AF4, Wyatt), a MALS detector (DAWN Heleos II, Wyatt), a UV detector  
484 (1260 Infinity G1314F, Agilent) and the separation channel (SC channel, PES membrane, cut-  
485 off 10 kDa, 490 μm spacer, wide type, Wyatt). Elution buffer: 1.15 g/L Na<sub>2</sub>HPO<sub>4</sub> (Merck),  
486 0.20 g/L NaH<sub>2</sub>PO<sub>4</sub> x H<sub>2</sub>O (Merck), 8.00 g/L NaCl (Sigma) and 0,20 g/L NaN<sub>3</sub> (Sigma),  
487 adjusted to pH 7.4, filtered through 0.1 μm. AF4 sequence (V<sub>x</sub> = cross flow in mL/min): (a)  
488 elution (2 min, V<sub>x</sub>: 1.0); (b) focus (1 min, V<sub>x</sub>: 1.0), focus + inject (1 min, V<sub>x</sub>: 1.0, inject flow:  
489 0.2 mL/min), repeated three times; (c) elution (30 min, linear V<sub>x</sub> gradient: 1.0 to 0.0); (d)  
490 elution (15 min, V<sub>x</sub>: 0.0); (e) elution + inject (5 min, V<sub>x</sub>: 0.0). A total protein mass of 17±0.3

491  $\mu\text{g}$  (Ifx, rhTNF $\alpha$  or ICs, respectively) was injected. The eluted sample concentration was  
492 calculated from the UV signal at 280 nm using extinction coefficients of 1.240 mL/(mg cm)  
493 or 1.450 mL/(mg cm) in the case of TNF $\alpha$  or Ifx, respectively. For the ICs, extinction  
494 coefficients were not available and difficult to calculate as the exact stoichiometry is not  
495 known. An extinction coefficient of 1.450 mL/(mg cm) was used for calculating the molar  
496 masses of all ICs. Especially in the case of ICs rich in TNF $\alpha$ , the true coefficients should be  
497 lower, and the molar masses of these complexes are overestimated by not more than 14 %.  
498 The determined molar masses for TNF $\alpha$ -rich complexes are therefore biased but the observed  
499 variations in molar mass for the different ICs remain valid. The mass-weighted mean of the  
500 distribution of molar masses for each sample was calculated using the ASTRA 7 software  
501 package (Wyatt).

502

503 *SLE patient cohort:* Sera from patients with SLE were obtained from the Immunologic,  
504 Rheumatologic Biobank (IR-B) of the Department of Rheumatology and Clinical  
505 Immunology. Biobanking and the project were approved by the local ethical committee of the  
506 University of Freiburg (votes 507/16 and 624/14). All patients who provided blood to the  
507 biobank had provided written informed consent. Ethical Statement: The study was designed in  
508 accordance with the guidelines of the Declaration of Helsinki (revised 2013). Patients with  
509 SLE ( $n = 25$ ) and healthy controls ( $n = 4$ ) were examined. All patients met the revised ACR  
510 classification criteria for SLE. Disease activity was assessed using the SLEDAI-2K score.  
511 C3d levels were analyzed in EDTA plasma using rocket double decker immune-  
512 electrophoresis with antisera against C3d (Polyclonal Rabbit Anti-Human C3d Complement,  
513 Agilent) and C3c (Polyclonal Rabbit Anti-Human C3c Complement Agilent) as previously  
514 described (72). Anti-human dsDNA antibodies titers were determined in serum using an anti-  
515 dsDNA IgG ELISA kit (diagnostik-a GmbH).

516

517 *Patient serum IC precipitation:* For polyethylene glycol (PEG) precipitation human sera were  
518 mixed with PEG 6000 (Sigma-Aldrich) in PBS at a final concentration of 10% PEG 6000.  
519 After overnight incubation at 4°C, ICs were precipitated by centrifugation at 2000 x g for  
520 30 min at 4 °C, pellets were washed once with PEG 6000 and then centrifugated at 2000 x g  
521 for 20 min at 4 °C. Supernatants were harvested and precipitates re-suspended in pre-warmed  
522 PBS for 1 h at 37 °C. IgG concentrations of serum, precipitates and supernatants obtained  
523 after precipitation were quantified by Nanodrop (Thermo Scientific™) measurement.

524  
525 *Mice and Models:* Animal experiments were approved by the local governmental commission  
526 for animal protection of Freiburg (Regierungspräsidium Freiburg, approval no. G16/59 and  
527 G19/21). Lupus-prone (NZBxNZW)F1 mice (NZB/WF1) were generated by crossing  
528 NZB/BINJ mice with NZW/LacJ mice, purchased from The Jackson Laboratory. KRNTg mice  
529 were obtained from F. Nimmerjahn (Universität Erlangen-Nürnberg) with the permission of  
530 D. Mathis and C. Benoist (Harvard Medical School, Boston, MA), C57BL/6 mice (BL/6) and  
531 NOD/ShiLtJArc (NOD/Lt) mice were obtained from the Charles River Laboratories. K/BxN  
532 (KRNTgxNOD)F1 mice (K/BxN) were obtained by crossing KRNTg mice and NOD/Lt mice.  
533 All mice were housed in a 12-h light/dark cycle, with food and water ad libitum. Mice were  
534 euthanized and blood collected for serum preparation from 16 weeks old BL/6 animals, from  
535 16 weeks old arthritic K/BxN animals and from 26 – 38 weeks old NZB/WF1 mice with  
536 established glomerulonephritis.

537  
538 *Statistical analyses:* Statistical analyses were performed using Graphpad Prism software (v6)  
539 and appropriate tests.

540

541

542

543 **Acknowledgements:** We thank T. Schleyer (IR-B Biobank) for providing patient samples.  
544 We are indebted to Falk. Nimmerjahn (Universität Erlangen-Nürnberg) for providing KRNtg  
545 mice. **Funding:** This work was supported by an intramural junior investigator fund of the  
546 Faculty of Medicine to PK (EQUIP - Funding for Medical Scientists, Faculty of Medicine,  
547 University of Freiburg), by the German Research foundation (DFG) (FOR2830 HE 2526/9-1)  
548 to HH, by the DFG research grant TRR130 to REV and the Ministry of Science, Research,  
549 and Arts Baden-Württemberg (Margarete von Wrangell Programm) to NC. **Author**  
550 **contributions:** HC and PK designed and developed the reporter system, conducted Fc-  
551 gamma receptor activation experiments and prepared synthetic immune complexes. AMP, US  
552 and REV manage the SLE patient cohort, provided sera and performed immune complex  
553 precipitation as well as IgG quantification. MH designed and performed AF4 analyses. NC  
554 manages the mouse models and provided sera. HH and PK supervised all experiments. HC  
555 and PK analysed and interpreted data. PK wrote the paper assisted by HC, AMP, MH, NC,  
556 REV and HH. **Competing interests:** The authors declare no financial and non-financial  
557 competing interests. **Data and materials availability:** All data associated with this study are  
558 present in the paper or Supplementary Materials.

559

560

## 561 **Supplementary Materials**

562 Fig. S1. rhTNF $\alpha$  is not toxic to mouse lymphocyte BW5147 cells even at high concentrations.

563 Fig. S2. AF4 elution profiles of Ifx/TNF $\alpha$ -immune complexes.

564 Table S1. Analysis of the molar mass distribution of ICs from AF4 data.

565

566 **References**

- 567 1. L. L. Lu, T. J. Suscovich, S. M. Fortune, G. Alter, Beyond binding: antibody effector  
568 functions in infectious diseases. *Nat Rev Immunol* **18**, 46-61 (2018).
- 569 2. J. V. Ravetch, S. Bolland, IgG Fc receptors. *Annu Rev Immunol* **19**, 275-290 (2001).
- 570 3. C. E. van der Poel, R. M. Spaapen, J. G. van de Winkel, J. H. Leusen, Functional  
571 characteristics of the high affinity IgG receptor, FcγRI. *J Immunol* **186**, 2699-  
572 2704 (2011).
- 573 4. P. Bruhns *et al.*, Specificity and affinity of human Fcγ receptors and their  
574 polymorphic variants for human IgG subclasses. *Blood* **113**, 3716-3725 (2009).
- 575 5. D. Urlaub *et al.*, Activation of natural killer cells by rituximab in granulomatosis with  
576 polyangiitis. *Arthritis Res Ther* **21**, 277 (2019).
- 577 6. A. Lux, X. Yu, C. N. Scanlan, F. Nimmerjahn, Impact of immune complex size and  
578 glycosylation on IgG binding to human FcγRI. *J Immunol* **190**, 4315-4323  
579 (2013).
- 580 7. F. Kiefer *et al.*, The Syk protein tyrosine kinase is essential for Fc gamma receptor  
581 signaling in macrophages and neutrophils. *Mol Cell Biol* **18**, 4209-4220 (1998).
- 582 8. Y. Luo, J. W. Pollard, A. Casadevall, Fcγ receptor cross-linking stimulates cell  
583 proliferation of macrophages via the ERK pathway. *J Biol Chem* **285**, 4232-4242  
584 (2010).
- 585 9. S. Greenberg, P. Chang, S. C. Silverstein, Tyrosine phosphorylation of the gamma  
586 subunit of Fc gamma receptors, p72syk, and paxillin during Fc receptor-mediated  
587 phagocytosis in macrophages. *J Biol Chem* **269**, 3897-3902 (1994).
- 588 10. S. Bournazos, T. T. Wang, R. Dahan, J. Maamary, J. V. Ravetch, Signaling by  
589 Antibodies: Recent Progress. *Annu Rev Immunol* **35**, 285-311 (2017).
- 590 11. F. Nimmerjahn, J. V. Ravetch, Antibody-mediated modulation of immune responses.  
591 *Immunol Rev* **236**, 265-275 (2010).
- 592 12. M. Heidelberger, F. E. Kendall, A Quantitative Study of the Precipitin Reaction  
593 between Type Iii Pneumococcus Polysaccharide and Purified Homologous Antibody.  
594 *J Exp Med* **50**, 809-823 (1929).
- 595 13. M. Heidelberger, F. E. Kendall, The Precipitin Reaction between Type Iii  
596 Pneumococcus Polysaccharide and Homologous Antibody : Iii. A Quantitative Study  
597 and a Theory of the Reaction Mechanism. *J Exp Med* **61**, 563-591 (1935).
- 598 14. A. M. Duchemin, L. K. Ernst, C. L. Anderson, Clustering of the High-Affinity Fc  
599 Receptor for Immunoglobulin-G (Fc-γ-Ri) Results in Phosphorylation of Its  
600 Associated γ-Chain. *J Biol Chem* **269**, 12111-12117 (1994).
- 601 15. A. Getahun, J. C. Cambier, Of ITIMs, ITAMs, and ITAMis: revisiting immunoglobulin  
602 Fc receptor signaling. *Immunol Rev* **268**, 66-73 (2015).
- 603 16. P. Bruhns, F. Jonsson, Mouse and human FcR effector functions. *Immunol Rev* **268**,  
604 25-51 (2015).
- 605 17. P. Bruhns, Properties of mouse and human IgG receptors and their contribution to  
606 disease models. *Blood* **119**, 5640-5649 (2012).
- 607 18. F. Nimmerjahn, J. V. Ravetch, Fcγ receptors as regulators of immune  
608 responses. *Nat Rev Immunol* **8**, 34-47 (2008).
- 609 19. F. Nimmerjahn, J. V. Ravetch, Fcγ receptors: old friends and new family  
610 members. *Immunity* **24**, 19-28 (2006).
- 611 20. M. Guilleams, P. Bruhns, Y. Saeys, H. Hammad, B. N. Lambrecht, The function of  
612 Fcγ receptors in dendritic cells and macrophages. *Nat Rev Immunol* **14**, 94-108  
613 (2014).
- 614 21. Z. K. Indik *et al.*, The high affinity Fc gamma receptor (CD64) induces phagocytosis in  
615 the absence of its cytoplasmic domain: the gamma subunit of Fc gamma RIIIA  
616 imparts phagocytic function to Fc gamma RI. *Exp Hematol* **22**, 599-606 (1994).
- 617 22. G. Fossati, R. C. Bucknall, S. W. Edwards, Insoluble and soluble immune complexes  
618 activate neutrophils by distinct activation mechanisms: changes in functional  
619 responses induced by priming with cytokines. *Ann Rheum Dis* **61**, 13-19 (2002).

- 620 23. J. J. Hubbard *et al.*, FcRn is a CD32a coreceptor that determines susceptibility to IgG  
621 immune complex-driven autoimmunity. *J Exp Med* **217**, (2020).
- 622 24. A. Pincetic *et al.*, Type I and type II Fc receptors regulate innate and adaptive  
623 immunity. *Nat Immunol* **15**, 707-716 (2014).
- 624 25. G. Vidarsson, G. Dekkers, T. Rispen, IgG subclasses and allotypes: from structure  
625 to effector functions. *Front Immunol* **5**, 520 (2014).
- 626 26. M. Z. Tay, K. Wiehe, J. Pollara, Antibody-Dependent Cellular Phagocytosis in  
627 Antiviral Immune Responses. *Front Immunol* **10**, 332 (2019).
- 628 27. E. A. Laborde *et al.*, Immune complexes inhibit differentiation, maturation, and  
629 function of human monocyte-derived dendritic cells. *J Immunol* **179**, 673-681 (2007).
- 630 28. S. Kang *et al.*, IgG-Immune Complexes Promote B Cell Memory by Inducing BAFF. *J*  
631 *Immunol* **196**, 196-206 (2016).
- 632 29. V. Granger, M. Peyneau, S. Chollet-Martin, L. de Chaisemartin, Neutrophil  
633 Extracellular Traps in Autoimmunity and Allergy: Immune Complexes at Work. *Front*  
634 *Immunol* **10**, 2824 (2019).
- 635 30. S. Berger, H. Ballo, H. J. Stutte, Immune complex-induced interleukin-6, interleukin-  
636 10 and prostaglandin secretion by human monocytes: A network of pro- and anti-  
637 inflammatory cytokines dependent on the antigen:antibody ratio. *Eur J Immunol* **26**,  
638 1297-1301 (1996).
- 639 31. L. Koenderman, Inside-Out Control of Fc-Receptors. *Front Immunol* **10**, 544 (2019).
- 640 32. R. Plomp *et al.*, Subclass-specific IgG glycosylation is associated with markers of  
641 inflammation and metabolic health. *Sci Rep* **7**, 12325 (2017).
- 642 33. T. C. Pierson *et al.*, The stoichiometry of antibody-mediated neutralization and  
643 enhancement of West Nile virus infection. *Cell Host Microbe* **1**, 135-145 (2007).
- 644 34. K. R. Patel, J. T. Roberts, A. W. Barb, Multiple Variables at the Leukocyte Cell  
645 Surface Impact Fc gamma Receptor-Dependent Mechanisms. *Front Immunol* **10**, 223  
646 (2019).
- 647 35. S. Bohm, D. Kao, F. Nimmerjahn, Sweet and sour: the role of glycosylation for the  
648 anti-inflammatory activity of immunoglobulin G. *Current topics in microbiology and*  
649 *immunology* **382**, 393-417 (2014).
- 650 36. R. J. Stopforth *et al.*, Detection of Experimental and Clinical Immune Complexes by  
651 Measuring SHIP-1 Recruitment to the Inhibitory FcgammaRIIB. *J Immunol* **200**, 1937-  
652 1950 (2018).
- 653 37. T. T. Wang, J. V. Ravetch, Immune complexes: not just an innocent bystander in  
654 chronic viral infection. *Immunity* **42**, 213-215 (2015).
- 655 38. D. H. Yamada *et al.*, Suppression of Fcgamma-receptor-mediated antibody effector  
656 function during persistent viral infection. *Immunity* **42**, 379-390 (2015).
- 657 39. U. Antes, H. P. Heinz, D. Schultz, D. Brackertz, M. Loos, C1q-bearing immune  
658 complexes detected by a monoclonal antibody to human C1q in rheumatoid arthritis  
659 sera and synovial fluids. *Rheumatol Int* **10**, 245-250 (1991).
- 660 40. R. H. Zubler *et al.*, Circulating and intra-articular immune complexes in patients with  
661 rheumatoid arthritis. Correlation of 125I-C1q binding activity with clinical and biological  
662 features of the disease. *J Clin Invest* **57**, 1308-1319 (1976).
- 663 41. D. Koffler, V. Agnello, R. Thoburn, H. G. Kunkel, Systemic lupus erythematosus:  
664 prototype of immune complex nephritis in man. *J Exp Med* **134**, 169-179 (1971).
- 665 42. T. V. Rajan, The Gell-Coombs classification of hypersensitivity reactions: a re-  
666 interpretation. *Trends in immunology* **24**, 376-379 (2003).
- 667 43. S. Tahir *et al.*, A CD153+CD4+ T follicular cell population with cell-senescence  
668 features plays a crucial role in lupus pathogenesis via osteopontin production. *J*  
669 *Immunol* **194**, 5725-5735 (2015).
- 670 44. A. Bano *et al.*, CD28 (null) CD4 T-cell expansions in autoimmune disease suggest a  
671 link with cytomegalovirus infection. *F1000Res* **8**, (2019).
- 672 45. E. Corrales-Aguilar *et al.*, A novel assay for detecting virus-specific antibodies  
673 triggering activation of Fcgamma receptors. *Journal of immunological methods* **387**,  
674 21-35 (2013).



- 675 46. H. A. D. Lagasse, H. Hengel, B. Golding, Z. E. Sauna, Fc-Fusion Drugs Have  
676 FcγR/C1q Binding and Signaling Properties That May Affect Their  
677 Immunogenicity. *AAPS J* **21**, 62 (2019).
- 678 47. S. Van den Hoecke *et al.*, Hierarchical and Redundant Roles of Activating  
679 FcγRs in Protection against Influenza Disease by M2e-Specific IgG1 and  
680 IgG2a Antibodies. *J Virol* **91**, (2017).
- 681 48. M. Tanaka *et al.*, Activation of FcγRI on monocytes triggers differentiation into  
682 immature dendritic cells that induce autoreactive T cell responses. *J Immunol* **183**,  
683 2349-2355 (2009).
- 684 49. S. Lisi, M. Sisto, D. D. Lofrumento, S. D'Amore, M. D'Amore, Advances in the  
685 understanding of the Fcγ receptors-mediated autoantibodies uptake. *Clin Exp*  
686 *Med* **11**, 1-10 (2011).
- 687 50. J. C. Anania, A. M. Chenoweth, B. D. Wines, P. M. Hogarth, The Human  
688 FcγRII (CD32) Family of Leukocyte FcR in Health and Disease. *Front Immunol*  
689 **10**, 464 (2019).
- 690 51. D. Metes *et al.*, Expression of functional CD32 molecules on human NK cells is  
691 determined by an allelic polymorphism of the FcγRIIC gene. *Blood* **91**, 2369-  
692 2380 (1998).
- 693 52. W. B. Breunis *et al.*, Copy number variation of the activating FCGR2C gene  
694 predisposes to idiopathic thrombocytopenic purpura. *Blood* **111**, 1029-1038 (2008).
- 695 53. F. Vuckovic *et al.*, Association of systemic lupus erythematosus with decreased  
696 immunosuppressive potential of the IgG glycome. *Arthritis Rheumatol* **67**, 2978-2989  
697 (2015).
- 698 54. Y. Kaneko, F. Nimmerjahn, J. V. Ravetch, Anti-inflammatory activity of  
699 immunoglobulin G resulting from Fc sialylation. *Science* **313**, 670-673 (2006).
- 700 55. P. Kolb *et al.*, Identification and Functional Characterization of a Novel Fcγ-  
701 Binding Glycoprotein in Rhesus Cytomegalovirus. *J Virol* **93**, (2019).
- 702 56. U. E. Nydegger, J. S. t. Davis, Soluble immune complexes in human disease. *CRC*  
703 *Crit Rev Clin Lab Sci* **12**, 123-170 (1980).
- 704 57. R. J. Levinsky, J. S. Cameron, J. F. Soothill, Serum immune complexes and disease  
705 activity in lupus nephritis. *Lancet* **1**, 564-567 (1977).
- 706 58. R. J. Levinsky, Role of circulating soluble immune complexes in disease. *Arch Dis*  
707 *Child* **53**, 96-99 (1978).
- 708 59. L. Briant, N. Coudronniere, V. Robert-Hebmann, M. Benkirane, C. Devaux, Binding of  
709 HIV-1 virions or gp120-anti-gp120 immune complexes to HIV-1-infected quiescent  
710 peripheral blood mononuclear cells reveals latent infection. *J Immunol* **156**, 3994-  
711 4004 (1996).
- 712 60. S. K. Oh *et al.*, Identification of HIV-1 envelope glycoprotein in the serum of AIDS and  
713 ARC patients. *J Acquir Immune Defic Syndr (1988)* **5**, 251-256 (1992).
- 714 61. D. A. Vuitton, L. Vuitton, E. Seilles, P. Galanaud, A plea for the pathogenic role of  
715 immune complexes in severe Covid-19. *Clin Immunol* **217**, 108493 (2020).
- 716 62. K. Madalinski, B. Burczynska, K. H. Heermann, A. Uy, W. H. Gerlich, Analysis of viral  
717 proteins in circulating immune complexes from chronic carriers of hepatitis B virus.  
718 *Clin Exp Immunol* **84**, 493-500 (1991).
- 719 63. D. A. Wetter, M. D. Davis, Lupus-like syndrome attributable to anti-tumor necrosis  
720 factor alpha therapy in 14 patients during an 8-year period at Mayo Clinic. *Mayo Clin*  
721 *Proc* **84**, 979-984 (2009).
- 722 64. D. A. MacDonald *et al.*, Aflibercept exhibits VEGF binding stoichiometry distinct from  
723 bevacizumab and does not support formation of immune-like complexes.  
724 *Angiogenesis* **19**, 389-406 (2016).
- 725 65. K. O. Saunders, Conceptual Approaches to Modulating Antibody Effector Functions  
726 and Circulation Half-Life. *Front Immunol* **10**, 1296 (2019).
- 727 66. T. Li *et al.*, Modulating IgG effector function by Fc glycan engineering. *Proceedings of*  
728 *the National Academy of Sciences of the United States of America* **114**, 3485-3490  
729 (2017).

- 730 67. M. R. Goodier *et al.*, Sustained Immune Complex-Mediated Reduction in CD16  
731 Expression after Vaccination Regulates NK Cell Function. *Front Immunol* **7**, 384  
732 (2016).
- 733 68. T. N. Mayadas, G. C. Tsokos, N. Tsuboi, Mechanisms of immune complex-mediated  
734 neutrophil recruitment and tissue injury. *Circulation* **120**, 2012-2024 (2009).
- 735 69. S. Nagarajan *et al.*, Cell-specific, activation-dependent regulation of neutrophil  
736 CD32A ligand-binding function. *Blood* **95**, 1069-1077 (2000).
- 737 70. K. Morizono *et al.*, Redirecting lentiviral vectors pseudotyped with Sindbis virus-  
738 derived envelope proteins to DC-SIGN by modification of N-linked glycans of  
739 envelope proteins. *J Virol* **84**, 6923-6934 (2010).
- 740 71. E. Corrales-Aguilar *et al.*, Human cytomegalovirus Fcγ binding proteins gp34  
741 and gp68 antagonize Fcγ receptors I, II and III. *PLoS pathogens* **10**, e1004131  
742 (2014).
- 743 72. E. Rother, B. Lang, R. Coldewey, K. Hartung, H. H. Peter, Complement split product  
744 C3d as an indicator of disease activity in systemic lupus erythematosus. *Clin*  
745 *Rheumatol* **12**, 31-35 (1993).

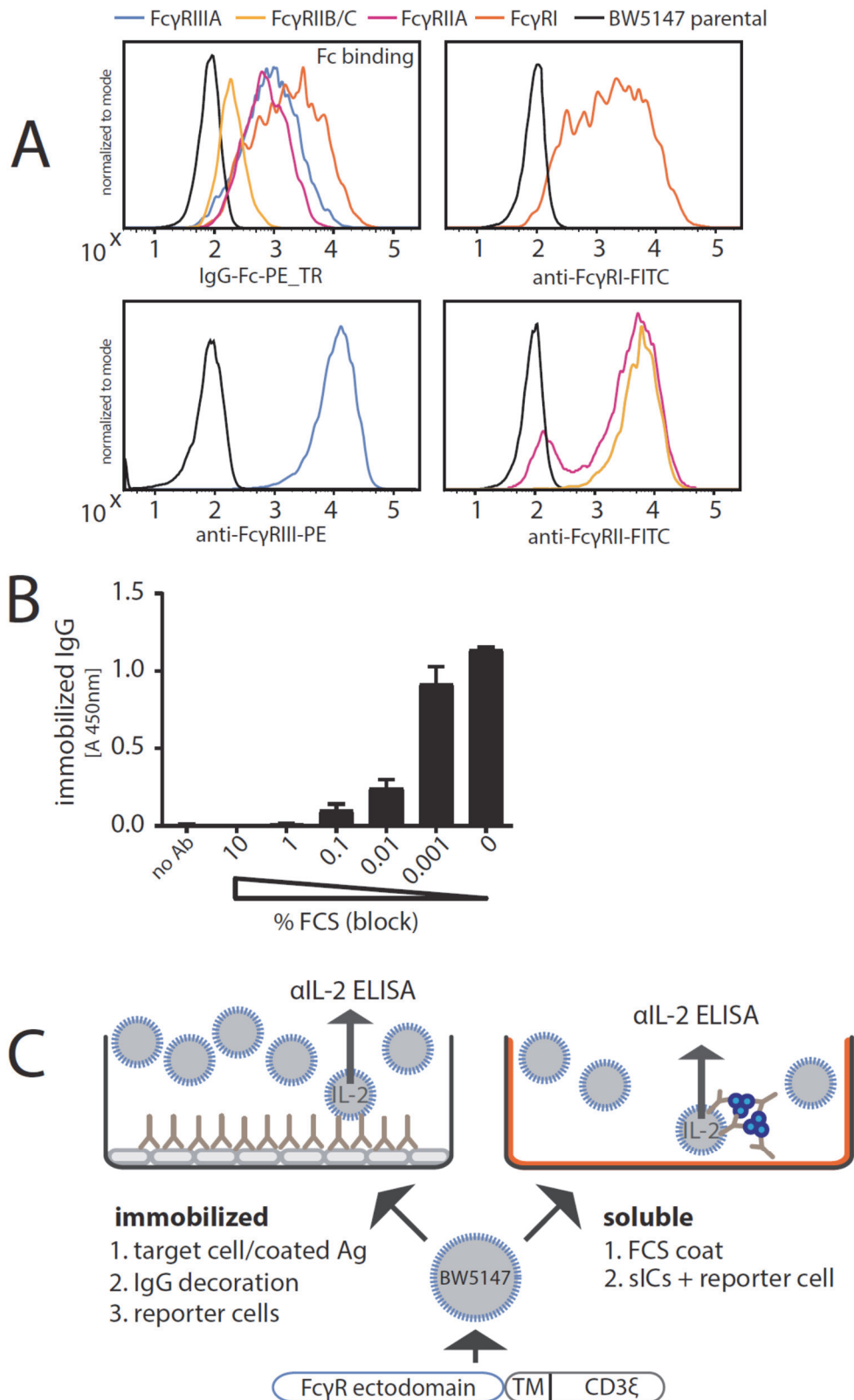
746

747

748 **Figures**

749

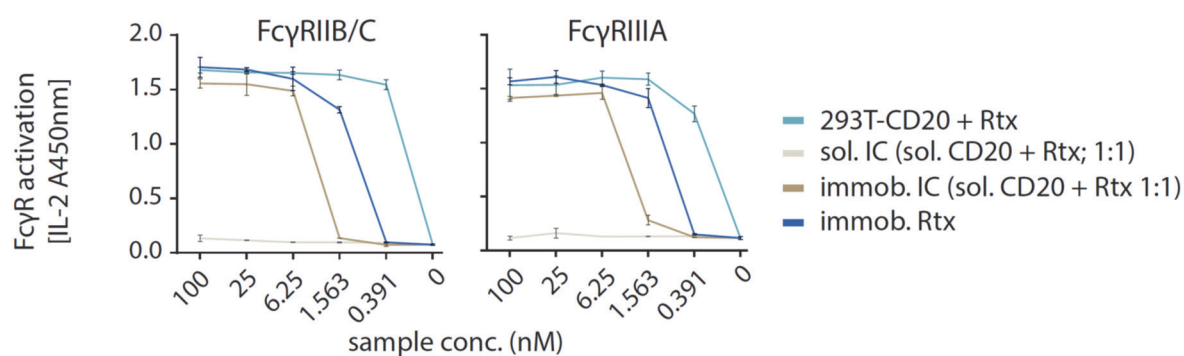
750 **Figure 1**



751

752

753 **Figure 2**

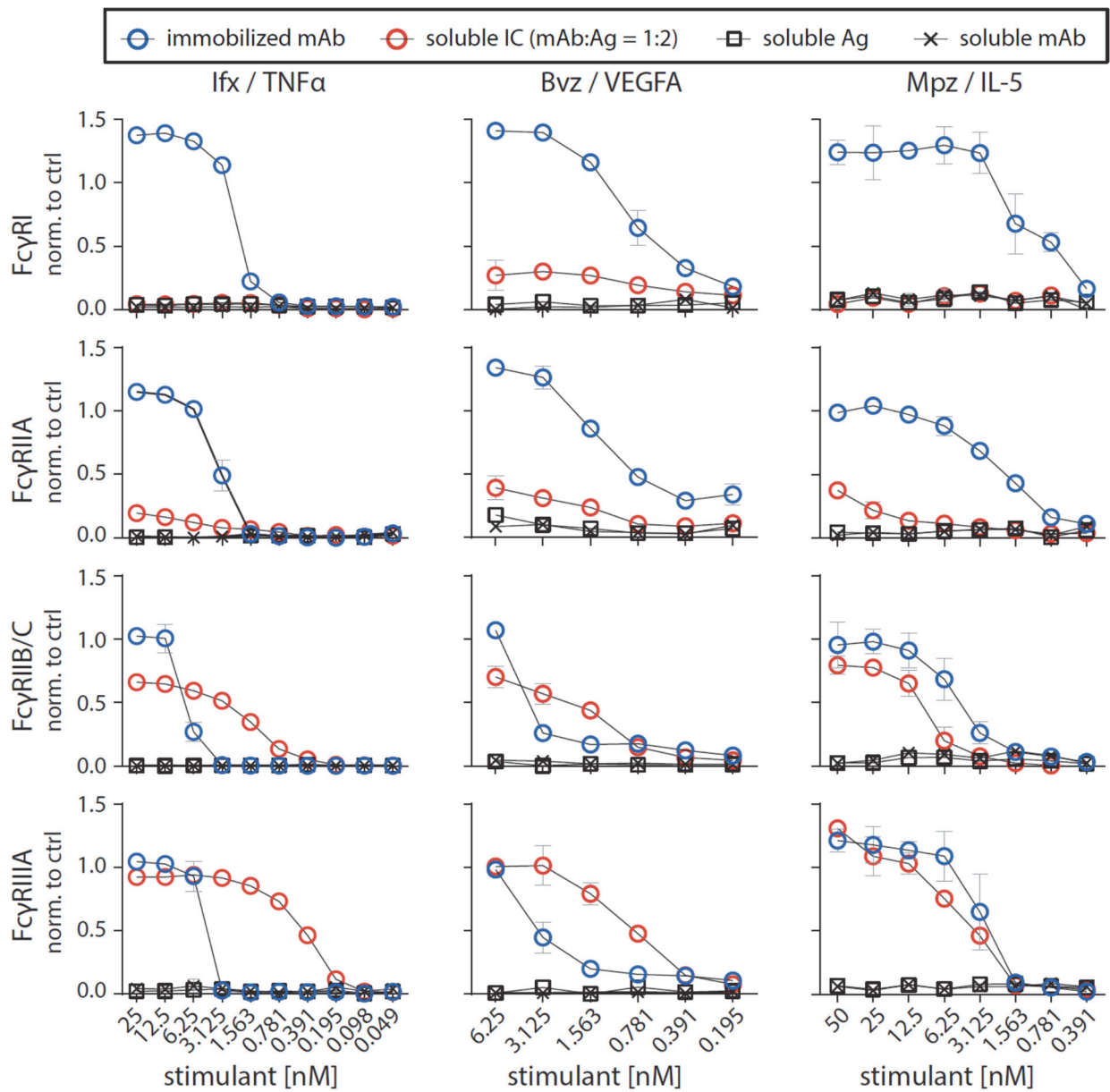


754

755 **Fig. 2. FcγRIIB/C and FcγRIIIA do not respond to small hetero-dimeric sICs but are**  
756 **sensitive to immobilized IgG/ICs.** Dose-dependent activation of FcγR-bearing reporter cells  
757 by immobilized IC can be mimicked by immobilized IgG. Response curves of human  
758 FcγRIIB/C and FcγRIIIA are similar between opsonized cells (293T cells stably expressing  
759 CD20 + Rtx), immobilized IC (rec. soluble CD20 + Rtx) and immobilized IgG (Rtx). sIC  
760 formed by monovalent antigen (rec. soluble CD20) do not activate human FcγRs. X-Axis  
761 shows sample concentration determined by antibody molarity. Y-Axis shows FcγR activation  
762 determined by reporter cell IL-2 production.

763

764 **Figure 3**



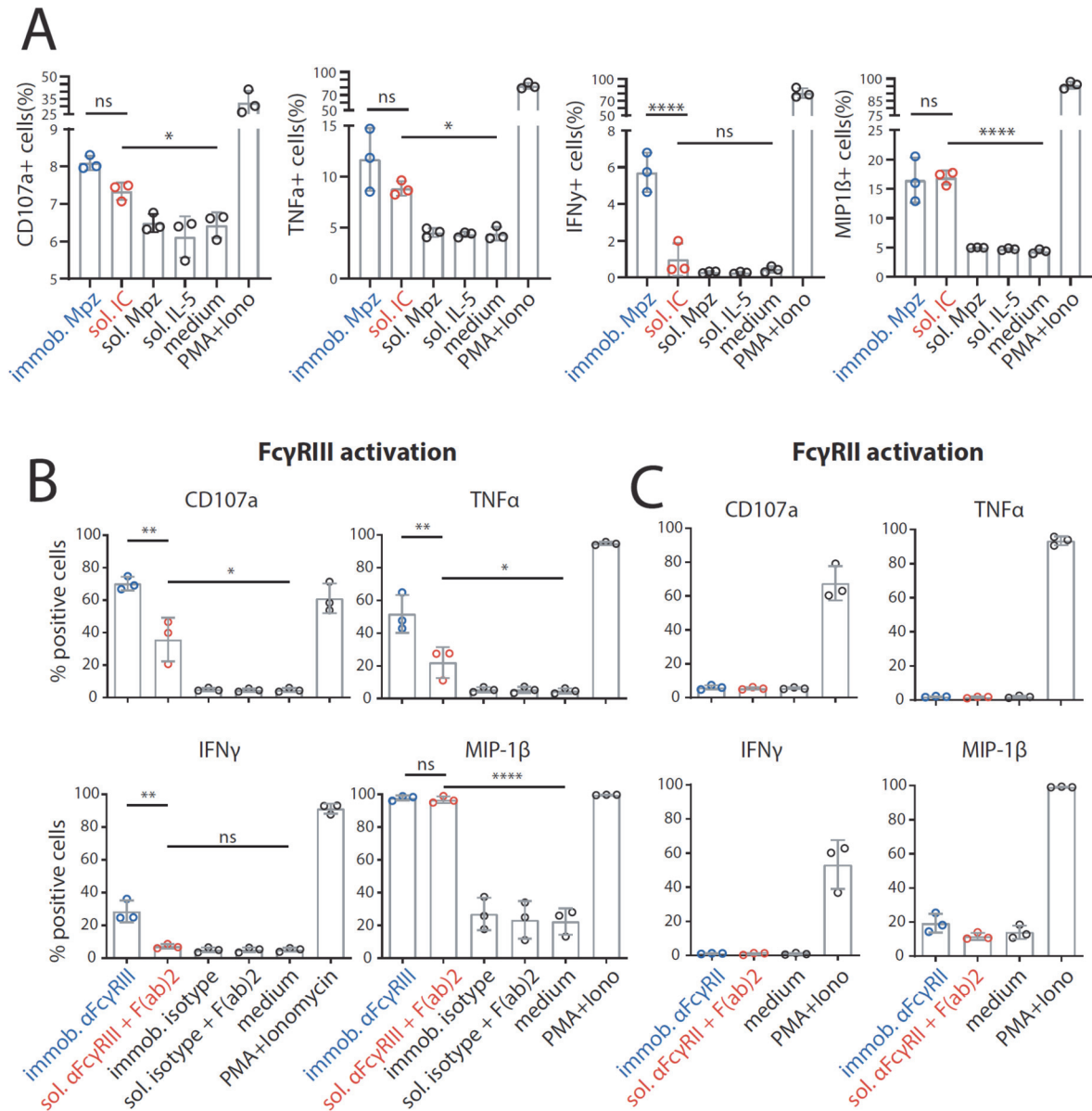
765  
766

767 **Fig. 3. FcγRIIB/C and FcγRIIIA are activated by sICs formed from multivalent**  
768 **antigens.** Three different multivalent ultra-pure antigens (Ag) mixed with respective therapy-  
769 grade mAbs were used to generate sICs as indicated for each set of graphs (top to bottom). IC  
770 pairs: infliximab (Ifx) and rhTNFα; mepolizumab (Mpz) and rhIL-5; bevacizumab (Bvz) and  
771 rhVEGFA. X-Axis: concentrations of stimulant expressed as molarity of either mAb or Ag  
772 monomer and IC (expressed as mAb molarity) at a mAb:Ag ratio of 1:2. Soluble antigen or  
773 soluble antibody alone served as negative controls and were not sufficient to activate human  
774 FcγRs. FcγR responses were normalized to immobilized rituximab (Rtx) at 1 μg/well (set to 1)  
775 and a medium control (set to 0). All FcγRs show dose-dependent activation towards  
776 immobilized IgG. FcγRIIA shows low activation at high sIC concentrations compared to  
777 immobilized IgG activation. FcγRI shows no activation towards sICs. FcγRIIIA and  
778 FcγRIIB/C are dose-dependently activated by sICs with responses comparable in strength to  
779 immobilized IgG stimulant. Experiments performed in technical replicates. Error bars = SD.  
780 Error bars smaller than symbols are not shown.

781 **Figure 4**

782

783



784

785

786

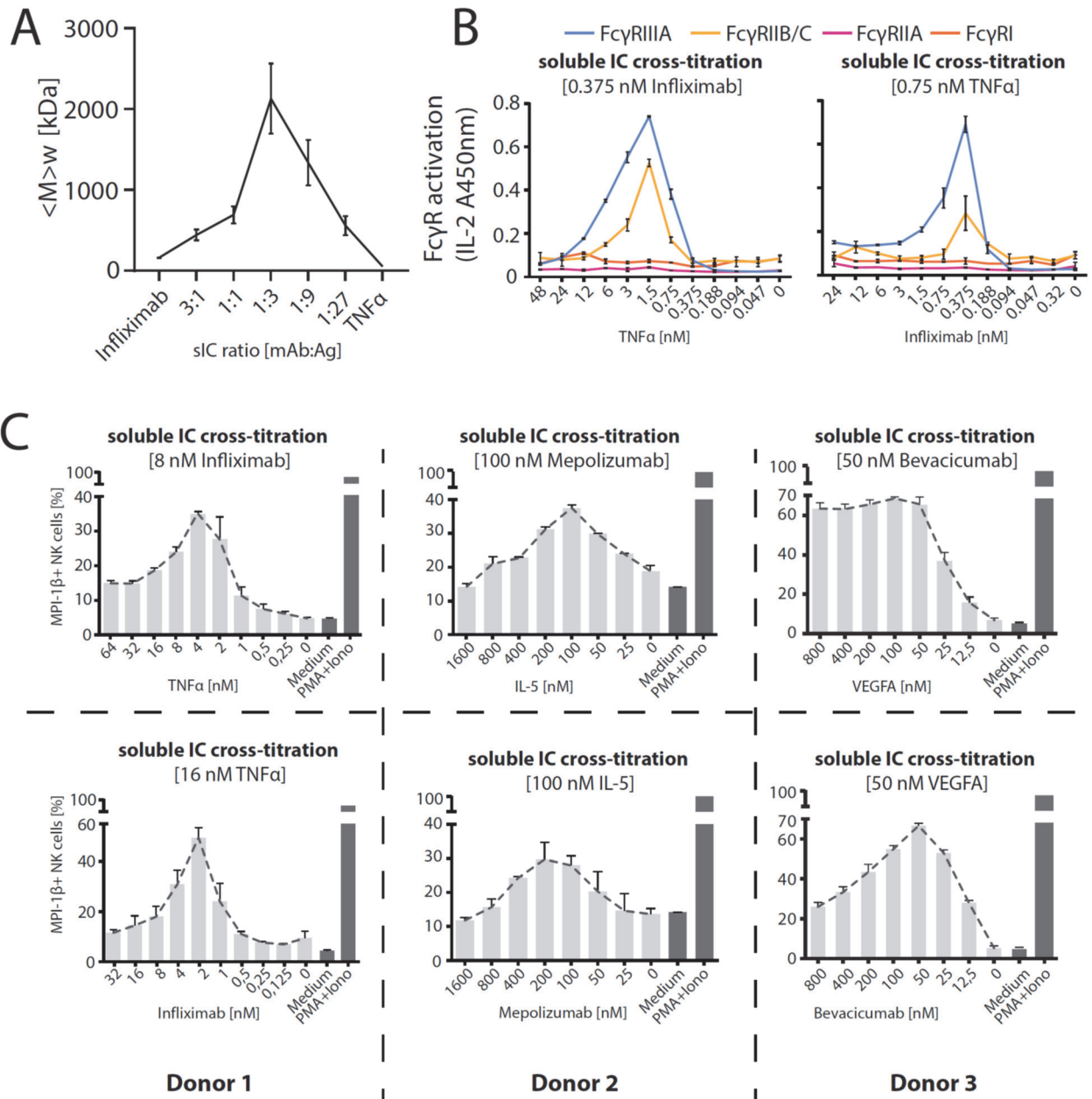
787 **Fig. 4. The FcγRIII-dependent activation pattern of primary NK cells depends on IC**  
788 **solubility.** Negatively selected primary NK cells purified from PBMCs of three healthy  
789 donors were tested for NK cell activation markers. Error bars = SD. Two-way ANOVA  
790 (Turkey). A) NK cells were incubated with immobilized IgG (mepolizumab, Mpz), soluble IC  
791 (Mpz:IL-5 = 1:1), soluble Mpz or soluble IL-5 (all at 200 nM, 10<sup>6</sup> cells). Incubation with  
792 PMA and Ionomycin (Iono) served as a positive control. Incubation with medium alone  
793 served as a negative control. B) NK cells were incubated for 4 h with immobilized FcγRIII-  
794 specific mAb, soluble mouse-anti-human IgG F(ab)<sub>2</sub> complexed FcγRIII-specific mAb  
795 (reverse sICs), immobilized IgG of non-FcγRIII-specificity (isotype control) or soluble F(ab)<sub>2</sub>  
796 complexed isotype control (all at 1 μg, 10<sup>6</sup> cells). Incubation with PMA and Ionomycin served  
797 as a positive control. Incubation with medium alone served as a negative control. C) As in B  
798 using an FcγRII-specific mAb. NK cells from the tested donors in this study do not react to  
799 FcγRII activation.



800 **Figure 5**

801

802

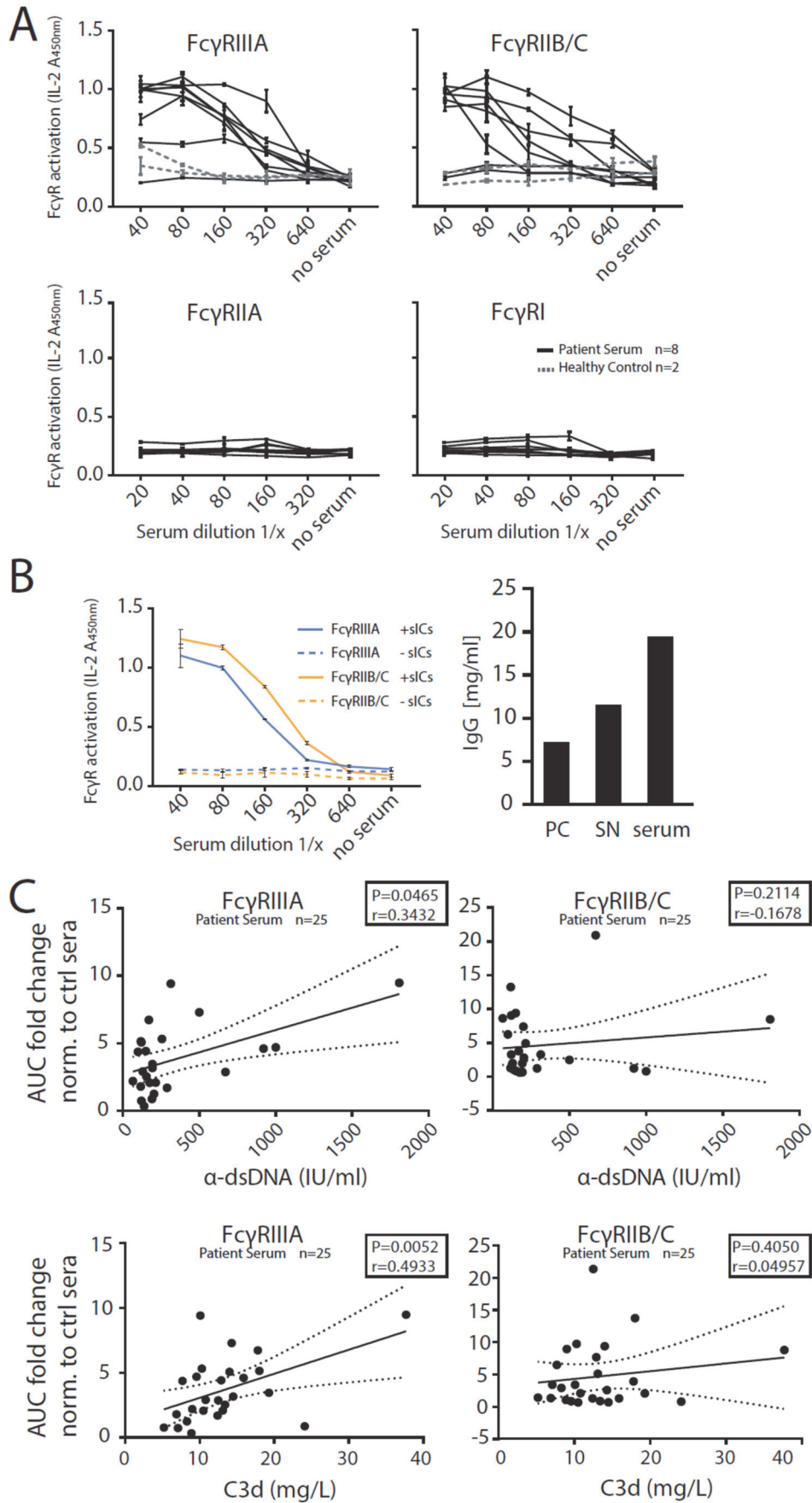


803

804

805 **Fig. 5. Fc $\gamma$ RIIB/C and Fc $\gamma$ R-IIIa respond to sIC size reproducing a Heidelberger-**  
806 **Kendall like precipitation curve.** A) infliximab (mAb) and rhTNF $\alpha$  (Ag) were mixed at  
807 different ratios (17  $\mu$ g total protein, calculated from monomer molarity) and analysed via  
808 AF4. sIC size is maximal at a 1:3 ratio of mAb:Ag and reduced when either mAb or Ag are  
809 given in excess.  $\langle M \rangle_w$  = mass-weighted mean of the molar mass distribution. Three  
810 independent experiments. Error bars = SD. Data taken from Table S1. One complete run  
811 analysis is shown in Fig. S2. B) Fc $\gamma$ R BW5147 reporter cell activation is sensitive to sIC size.  
812 sICs of different size were generated by cross-titration according to the AF4 determination.  
813 Reporter cells were incubated with fixed amounts of either mAb (infliximab, left) or Ag  
814 (rhTNF $\alpha$ , right) and titrated amounts of antigen or antibody, respectively. X-Axis shows  
815 titration of either antigen or antibody, respectively (TNF $\alpha$  calculated as monomer). IL-2  
816 production of reporter cells shows a peak for Fc $\gamma$ RIIB/C and Fc $\gamma$ RIIIa activation at an  
817 antibody:antigen ratio between 1:2 and 1:4. Fc $\gamma$ Rs I and IIA show no activation towards sICs  
818 in line with previous observations, see Fig.3. Two independent experiments. Error bars = SD.  
819 C) Purified primary NK cells from three different donors were incubated with cross-titrated  
820 sICs as in A. NK cells were measured for MIP-1 $\beta$  expression (% positivity). Incubation with  
821 PMA and Ionomycin served as a positive control. Incubation with medium alone served as a  
822 negative control. Measured in technical replicates. Error bars = SD.

823 **Figure 6**



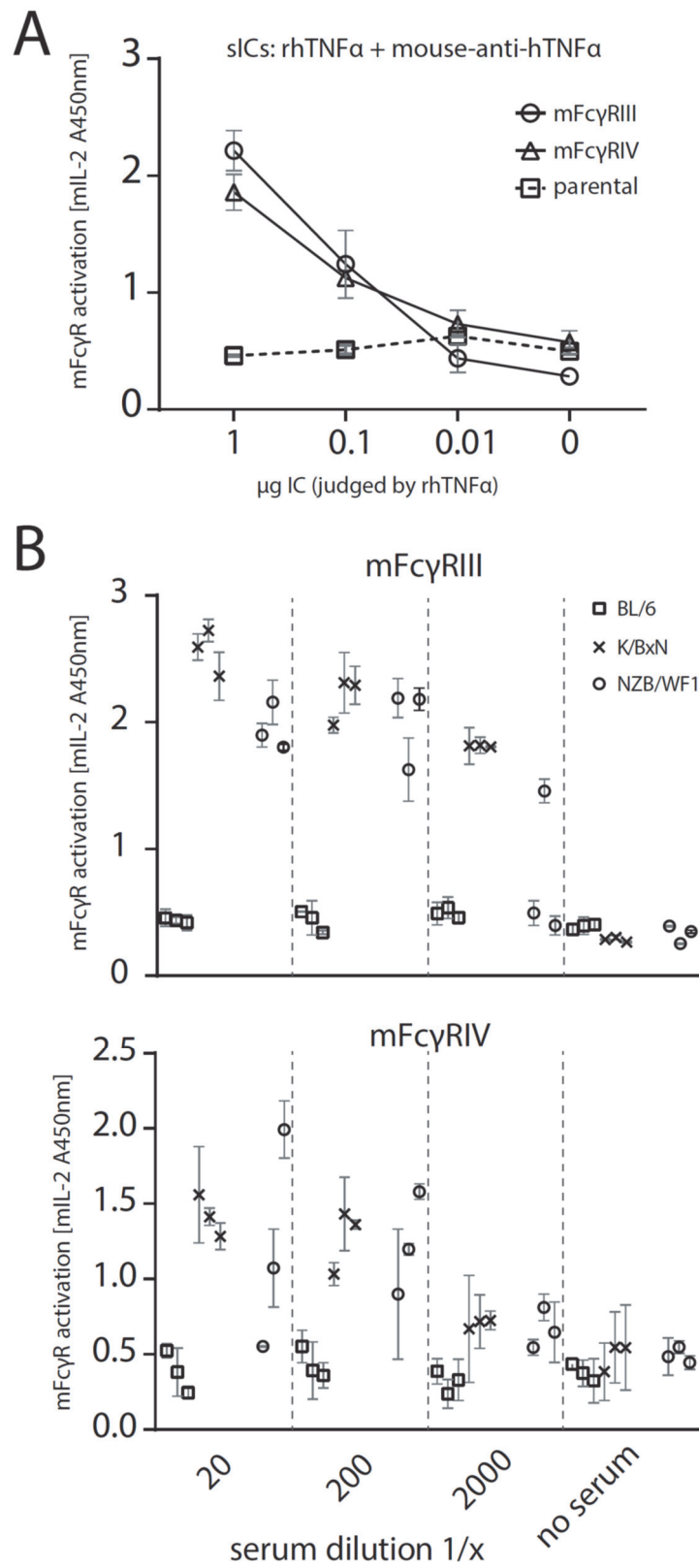
825 **Fig. 6. The reporter assay enables quantification of serum-derived sICs from SLE**  
826 **patients.** Serum derived sIC from systemic lupus erythematosus (SLE) patients activate  
827 human Fc $\gamma$ R reporter cells. 25 patients and 4 healthy control individuals were separated into  
828 three groups for measurement. A) Experiments shown for an exemplary group of 8 SLE  
829 patients and two healthy individuals. Dose-dependent reactivity of Fc $\gamma$ Rs IIIA and IIB/C was  
830 observed only for SLE patient sera and not for sera from healthy individuals. Fc $\gamma$ Rs I and IIA  
831 show no reactivity towards clinical IC in line with previous observations. B) Activation of  
832 Fc $\gamma$ Rs IIB/C and IIIA by patient serum is mediated by serum derived sICs. Patient serum  
833 samples were depleted of sICs by PEG precipitation and the supernatant (SN) was compared  
834 to untreated serum regarding Fc $\gamma$ R activation (left). Performed in technical replicates. IgG  
835 concentration in the precipitate (PC), supernatant (SN) or unfractionated serum respectively is  
836 shown in the bar graph (right). IC precipitation did leave non-complexed IgG in the  
837 supernatant. C) Fc $\gamma$ RIIIA activation, but not Fc $\gamma$ RIIB/C activation, significantly correlates  
838 with known SLE disease markers. Fc $\gamma$ R activation data from A was correlated to established  
839 SLE disease markers ( $\alpha$ -dsDNA levels indicated as IU/ml or C3d concentrations indicated as  
840 mg/L). Fc $\gamma$ R activation from a dose-response curve as in A was calculated as area under curve  
841 (AUC) for each SLE patient (n=25) or healthy individual (n=4) and expressed as fold change  
842 compared to the healthy control mean. SLE patients with  $\alpha$ -dsDNA levels below 50 IU/ml  
843 and C3d values below 6 mg/L were excluded. One-tailed Spearman's.

844

845

846 **Figure 7**

847



848

849

850 **Fig. 7. The reporter assay can be applied to mouse models of autoimmune disease. A)**

851 Reporter cells expressing mFcγRIII, mFcγRIV or parental BW5147 cells were incubated with

852 titrated amounts of synthetic sICs generated from rhTNFα and mouse-anti-hTNFα at a 1:1

853 ratio by mass. One experiment in technical replicates. Error bars = SD. B) Titrations of 3

854 mouse sera per group (C57BL/6, K/BxN or NZB/WF1) were incubated with mFcγR reporter

855 cells and FcγR activation was assessed as described above. Sera from BL/6 mice served as

856 negative control. Performed in technical replicates. Error bars = SD.

857

858

859

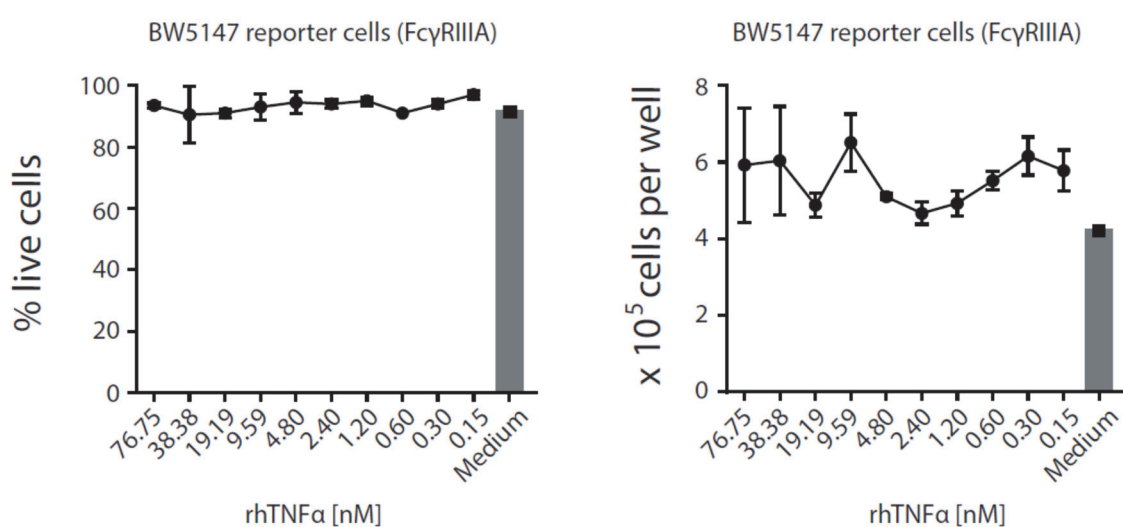
## -Supplementary Material-

860

861 **Figure S1**

862

863



864

865 **Fig. S1. rhTNFα is not toxic to mouse lymphocyte BW5147 cells even at high**

866 **concentrations.** Cell count and percentage of live cells were unaltered over a 16 h time frame

867 of reporter cell culture in the presence of indicated rhTNFα concentrations and comparable to

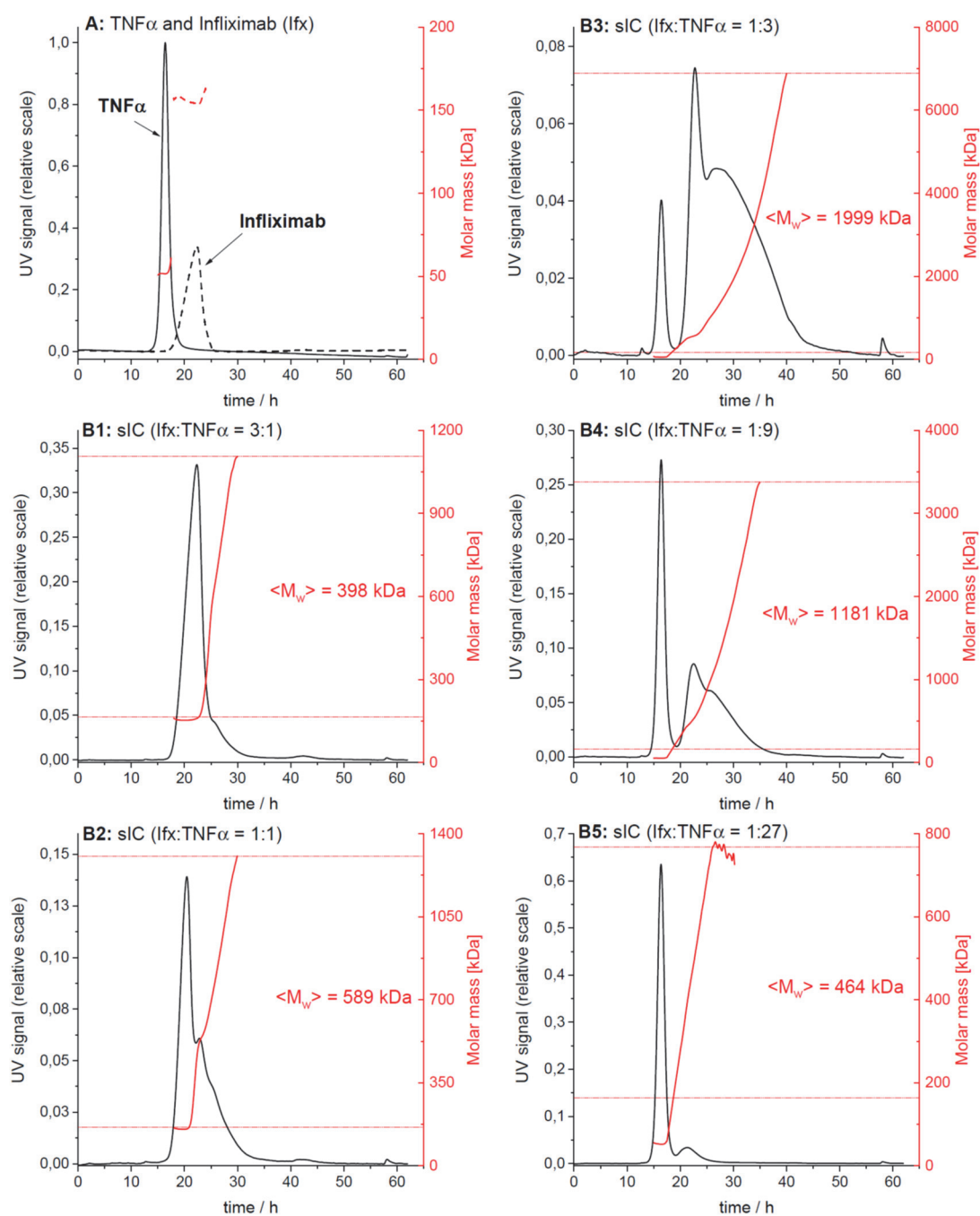
868 regular growth in complete medium. Experiments were conducted in 3 replicates. Error bars =

869 SD.

870

871 **Figure S2**

872



873

874



875 **Fig. S2. AF4 elution profiles of Ifx/TNF $\alpha$ -immune complexes.**

876 The elution profiles from one of three independent runs are shown. Protein concentration in  
 877 the eluate is shown in black (UV signal at  $\lambda = 280$  nm, normalized to the highest UV signal  
 878 found in this experiment), molar masses determined by MALS for a given retention time in  
 879 red. Horizontal red lines indicate the range of molar masses used to calculate the mass-  
 880 weighted mean of molar masses  $\langle M_w \rangle$ . A) Overlay of the elution profiles obtained for TNF $\alpha$   
 881 and Ifx, respectively; B1 to B5) Elution profiles for sICs formed after incubation of TNF $\alpha$  and  
 882 Ifx at different molar ratios.

883

884 **Table S1**

| Sample           | Range of assigned molar masses [kDa] |                                    |                                    | Mass-weighted mean of assigned molar masses [kDa] |                              |                              |  |
|------------------|--------------------------------------|------------------------------------|------------------------------------|---|------------------------------|------------------------------|--|
|                  | Run 1                                | Run 2                              | Run 3                              | Run 1   | Run 2                        | Run 3                        | Mean $\pm$ SD                          |
| Infliximab, IFX  | 158 – 182                            | 153 – 164                          | 159 – 193                          | 162   | 156                          | 163                          | 160 $\pm$ 4                            |
| TNF -alpha       | 52 – 55                              | 51 – 61                            | 52 – 62                            | 52  | 52                           | 52                           | 52 $\pm$ 0                             |
| Immune complexes |                                      |                                    |                                    |   |                              |                              |  |
| IFX/TNF 3:1      | 182 – 1.16 $\cdot$ 10 <sup>3</sup>   | 164 – 1.11 $\cdot$ 10 <sup>3</sup> | 193 – 1.10 $\cdot$ 10 <sup>3</sup> | 409   | 398                          | 518                          | 442 $\pm$ 66                           |
| IFX/TNF 1:1      | 182 – 2.06 $\cdot$ 10 <sup>3</sup>   | 164 – 1.31 $\cdot$ 10 <sup>3</sup> | 193 – 1.42 $\cdot$ 10 <sup>3</sup> | 801   | 589                          | 681                          | 690 $\pm$ 106                          |
| IFX/TNF 1:3      | 182 – 5.05 $\cdot$ 10 <sup>3</sup>   | 164 – 6.89 $\cdot$ 10 <sup>3</sup> | 193 – 10.8 $\cdot$ 10 <sup>3</sup> | 1.77 $\cdot$ 10 <sup>3</sup>                      | 2.00 $\cdot$ 10 <sup>3</sup> | 2.61 $\cdot$ 10 <sup>3</sup> | 2.13 $\cdot$ 10 <sup>3</sup> $\pm$ 435 |
| IFX/TNF 1:9      | 182 – 5.36 $\cdot$ 10 <sup>3</sup>   | 164 – 3.38 $\cdot$ 10 <sup>3</sup> | 193 – 3.51 $\cdot$ 10 <sup>3</sup> | 1.66 $\cdot$ 10 <sup>3</sup>                      | 1.18 $\cdot$ 10 <sup>3</sup> | 1.17 $\cdot$ 10 <sup>3</sup> | 1.34 $\cdot$ 10 <sup>3</sup> $\pm$ 279 |
| IFX/TNF 1:27     | 182 – 1.68 $\cdot$ 10 <sup>3</sup>   | 164 – 768                          | 193 – 1.01 $\cdot$ 10 <sup>3</sup> | 689   | 464                          | 521                          | 558 $\pm$ 117                          |

885

886 **Table S1. Analysis of the molar mass distribution of ICs from AF4 data.**

887 For a given elution time, the AF4 profiles provide the concentration (UV) at which a given  
 888 molar mass (MALS) of a protein is present in the sample. The molar mass distribution of Ifx,  
 889 TNF $\alpha$  and their immune complexes (sICs) was obtained by plotting the cumulative frequency  
 890 as a function of molar mass. For a selected range of molar masses, a mass-weighted mean  
 891 value ( $\langle M_w \rangle$ ) was calculated. All detected molar masses were selected in the case of Ifx and  
 892 TNF $\alpha$  whereas only molar masses larger than the maximal molar mass found for Ifx were  
 893 assigned to sICs. The table shows the range of assigned molar masses and the calculated  
 894  $\langle M_w \rangle$  for each AF4 run (n = 3).